

# Evidence for a two-phase Palmer Land event from crosscutting structural relationships and emplacement timing of the Lassiter Coast Intrusive Suite, Antarctic Peninsula: Implications for mid-Cretaceous Southern Ocean plate configuration

Alan P. M. Vaughan,<sup>1</sup> Graeme Eagles,<sup>2</sup> and Michael J. Flowerdew<sup>1</sup>

Received 10 August 2011; revised 29 November 2011; accepted 12 December 2011; published 9 February 2012.

[1] New analysis of the relationships between geological structural data and radiometric ages for the Lassiter Coast Intrusive Suite indicate that the collisional mid-Cretaceous Palmer Land Event orogeny in the Antarctic Peninsula has had two kinematic phases, forming an intersection orocline, one of which can be related to Cretaceous Southern Ocean plate motions. Both are compressional phases along the Eastern Palmer Land Shear Zone: Phase 1 occurred at ~107 Ma with a principal paleostrain axis of 341°, and is best expressed in southern Palmer Land although evident elsewhere on the Antarctic Peninsula; Phase 2 occurred at ~103 Ma with a principal paleostrain axis of 259.5°, but is confined to between 68°S and 74°S. A peak in Lassiter Coast Intrusive Suite magma emplacement rate was coeval with Phase 1, whereas Phase 2 may have coincided with a lull. During Phase 1, the allochthonous Central and Western Domain terranes may have been transported to the Gondwana margin, represented by the para-autochthonous Eastern Domain, on board the Phoenix plate or on board the South American plate. The variable provenance indicators from the Central and Western terranes can be cited to support either, or a combination, of these scenarios. The convergence direction evident from Phase 2 structures cannot easily be reproduced in regional plate kinematic models. This, and the localized evidence for superposition of Phase 2 structures on Phase 1 structures suggests that Phase 2 is unlikely to have occurred solely in response to changes in the kinematics of the large plates considered.

**Citation:** Vaughan, A. P. M., G. Eagles, and M. J. Flowerdew (2012), Evidence for a two-phase Palmer Land event from crosscutting structural relationships and emplacement timing of the Lassiter Coast Intrusive Suite, Antarctic Peninsula: Implications for mid-Cretaceous Southern Ocean plate configuration, *Tectonics*, 31, TC1010, doi:10.1029/2011TC003006.

## 1. Introduction

[2] The mid-Cretaceous interval (Barremian to Turonian; 130–88 Ma [Gradstein *et al.*, 2004]) is a time of significant magmatic, tectonic and paleoenvironmental change [Larson, 1995]. It is marked by high rates of magmatism, accelerated plate motions [Seton *et al.*, 2009], paleo-Pacific basin plate reorganization [Sager, 2006] and unusual stability of the geomagnetic field [e.g., Biggin and Thomas, 2003]. In the paleo-Pacific basin, mid-Cretaceous events include Pacific-Phoenix-Farallon spreading system reorganization and eruption of three large igneous provinces [Worthington *et al.*, 2006], enhanced subduction-related magmatism, and widespread short-lived intense deformation [e.g., Vaughan and Livermore, 2005].

[3] On the West Gondwana margin [Vaughan and Pankhurst, 2008], mid-Cretaceous deformation structures are developed from southern South America [e.g., Arancibia, 2004; Kraemer, 2003] to Marie Byrd Land [Siddoway *et al.*, 2005]. The expression of tectonism varies along the margin, with, for example, extension associated with rifting-off of New Zealand [e.g., Siddoway *et al.*, 2005] in the main part of West Antarctica but collisional orogenesis in the Antarctic Peninsula [e.g., Vaughan and Livermore, 2005]. Here, this was associated with the accretion of allochthonous terranes to the Gondwana margin [Vaughan and Pankhurst, 2008]. It produced an oroclinal deformation zone during the Palmer Land Event [Kellogg and Rowley, 1989; Vaughan and Storey, 2000] between 110 and 100 Ma [Vaughan *et al.*, 2002a; Vaughan *et al.*, 2002b]. Previous research has raised questions over the origin of this orocline [Grunow, 1993; Hamilton, 1967; Kellogg, 1980] and these are addressed here.

[4] Dating of deformation structures by U-Pb zircon and Ar-Ar laser techniques gave ages of ~107 Ma [Vaughan *et al.*, 2002a] and ~103 Ma [Vaughan *et al.*, 2002b], respectively, which were within statistical error of each other

<sup>1</sup>British Antarctic Survey, Cambridge, UK.

<sup>2</sup>Department of Earth Sciences, Royal Holloway, University of London, Egham, UK.

and interpreted as a single mid-Cretaceous event [Vaughan and Livermore, 2005]. However, a re-examination of the age data in light of detailed structural analysis, presented here, indicates that the two radiometric ages date separate two phases of the event with distinct kinematics and paleostress directions, indicating extreme changes in finite strain axes in an interval of less than 4 million years.

[5] Mid-Cretaceous magmatism is expressed as emplacement of large volume plutonic complexes, which in the Antarctic Peninsula are represented by the Lassiter Coast Intrusive Suite (LCIS) [Rowley et al., 1983; Vennum and Rowley, 1986], a voluminous suite of more than 60 mafic to felsic calc-alkaline plutons emplaced over an area of  $800 \times 100$  km between 120 and 95 Ma but with a major peak in plutonism between 110 and 100 Ma, approximately coincident with the Palmer Land Event. Here we show a complex relationship between collisional orogenesis during the Palmer Land Event and the timing of magmatism.

[6] This paper builds on earlier work [Vaughan and Storey, 2000; Vaughan et al., 2002a; Vaughan et al., 2002b], incorporating data from new localities in the eastern Antarctic Peninsula. It outlines the evidence for a two phase Palmer Land Event and links onshore structural synthesis with a new plate kinematic interpretation to place the first phase of a polyphase Palmer Land Event in its plate kinematic framework, shed new light on the processes of terrane collision with the Gondwana margin, and resolve conflicting structural interpretations between the Antarctic Peninsula and southern South America.

## 2. Geological Setting

[7] The study area comprises the southern Antarctic Peninsula, in particular Palmer Land (Figure 1). Physiographically, the area comprises a large arc, over 1000 km long, facing the Pacific margin, with the trend of its long axis ranging from southwesterly in the southern part and curving smoothly to northerly in its northern part. Topographically it forms a large plateau of the order of 1000 m high on average, but with higher mountain ranges in its eastern part including Mount Jackson at 3184 m and other large ranges with peaks in excess of 2500 m such as in the Welsh Mountains and the Eternity Range. The eastern ranges are roughly located along the trend of the ductile Eastern Palmer Land Shear Zone (EPLSZ), a major terrane-bounding fault and oblique-reverse to reverse deformation zone up to 20 km-wide identified by Vaughan and Storey [2000]. This structure is exposed for over 1500 km in Palmer Land, and may form a major structural boundary for over 3000 km between para-autochthonous rocks of the Gondwana margin and allochthonous terranes, from Thurston Island to the South Shetland Islands (Figure 1). Oblique-dextral reverse where it strikes E-W in southern Palmer Land, it swings to approximately N-S orientation in eastern Palmer Land where it is developed as a broad reverse mylonite zone with abundant SL-, L- and LS-fabrics [Vaughan and Storey, 2000].

[8] Geologically, the field area is part of the late Paleozoic to Mesozoic magmatic arc that makes up the Antarctic Peninsula [e.g., Millar et al., 2002; Storey and Garrett, 1985]. Building on the early recognition of its subduction-

related origin [Smellie, 1981; Suárez, 1976], Vaughan and Storey [2000] subdivided it into tectonostratigraphic terranes [Vaughan et al., 2005] following discovery of the collisional EPLSZ [Vaughan and Storey, 2000].

[9] After Vaughan and Storey [2000], the Antarctic Peninsula region can be subdivided into at least seven terranes, or sub-terranes, grouped into three major domains (Figure 1). The Western Domain consists of accretionary complex turbiditic sandstones with allochthonous oceanic basalts and sediments [Doubleday and Tranter, 1994] of predominantly Jurassic and Cretaceous age of the LeMay Group [Holdsworth and Nell, 1992] and the Scotia Metamorphic Complex [Trouw et al., 2000]; however, some significant Triassic tracts crop out on Alexander Island [Willan, 2003] and the oldest rocks known are late Carboniferous-Permian fossiliferous sandstones in eastern Alexander Island [Kelly et al., 2001]. The accretionary complex rocks of Alexander Island form the basement to an important fore-arc basin sequence, the Fossil Bluff Group, deposited from early mid-Jurassic to mid-Cretaceous Albian times [Doubleday et al., 1993; Macdonald et al., 1999].

[10] The Central Domain is separated from the Western Domain by George VI Sound [Vaughan and Storey, 2000] and seismic data image a low-angle detachment beneath the sound dipping west consistent with a major tectonic boundary [Bell and King, 1998]. The Central Domain is a largely magmatic arc terrane with abundant plutonic and volcanic components ranging from Silurian to Cretaceous age [Millar et al., 2002; Vaughan and Storey, 2000]. Based on recent aerogeophysical data it can be subdivided into an eastern and western zone in Palmer Land [Ferraccioli et al., 2006] (Figure 1), interpreted as dominantly felsic and dominantly mafic arc sub-domains respectively.

[11] The Eastern Domain is separated from the Central Domain by the EPLSZ, described above. The Eastern Domain appears to represent the extended Late Paleozoic margin of Gondwana [Ferris et al., 2002] forming the basement to large Mesozoic sedimentary basins that host voluminous Gondwana break-up silicic volcanic rocks [Hunter et al., 2006; Riley et al., 2001] and the Latady Group [Hunter and Cantrill, 2006] and Larsen Basin [Hathway, 2000] marine clastic sequences. The later Paleozoic sedimentary part of this Gondwana sequence contains Glossopteris-bearing Permian sandstones [Gee, 1989; Laudon, 1991]. The Eastern Domain also hosts the voluminous calc-alkaline plutonic rocks of the LCIS [Rowley et al., 1983; Vennum and Rowley, 1986].

[12] Structures of the Palmer Land Event are widely developed through the domains of the southern Antarctic Peninsula and variably overprint earlier structures, for example from Triassic deformation [Vaughan and Livermore, 2005]. In the Western Domain on Alexander Island the tectonic event is expressed as general uplift and termination of deposition of the Fossil Bluff Group [Storey et al., 1996] and thrusting associated with dextral transpression [Doubleday and Storey, 1998]. In the Central Domain in Palmer Land, evidence for uplift and exhumation is also present [Leat et al., 2009] as well as brittle-ductile thrusting and transpressional shearing that affected crystalline plutonic and metamorphic rocks [Vaughan et al., 1999]. In the Eastern Domain, the tectonic event is most fully developed as ductile shearing of metamorphic and crystalline rocks [Vaughan et al., 2002b;

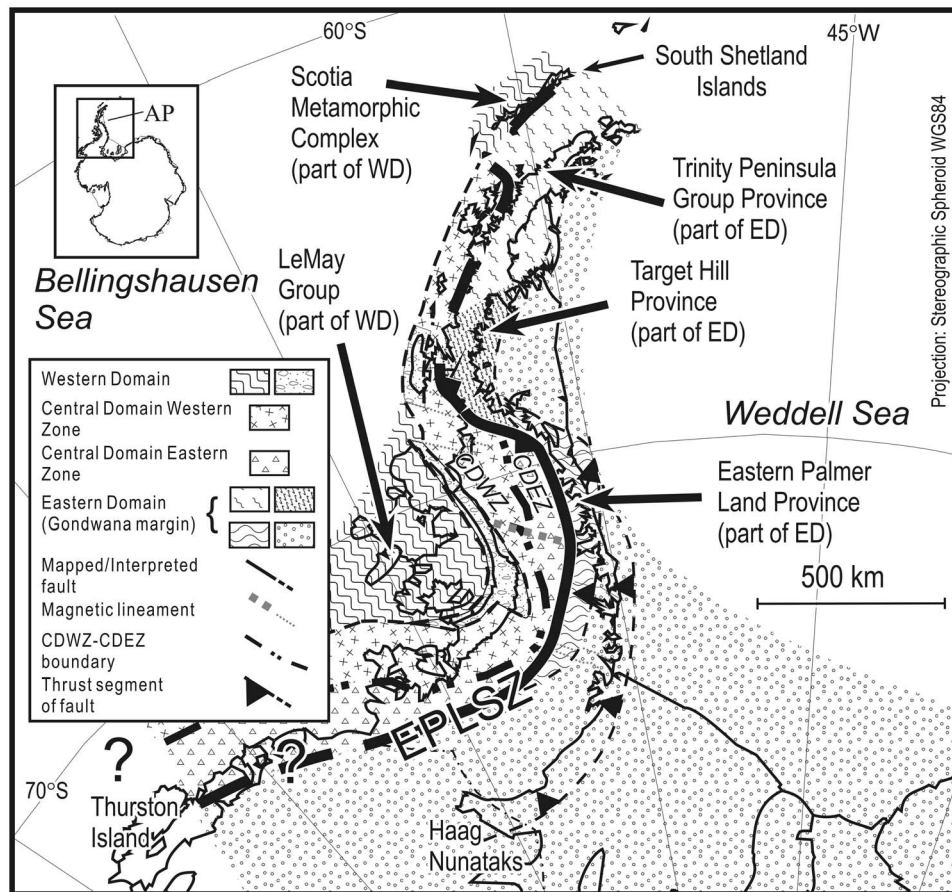


**Figure 1.** Tectonic elements map for the Antarctic Peninsula after *Vaughan and Storey* [2000] and *Ferraccioli et al.* [2006]. EPLSZ is Eastern Palmer Land Shear Zone.

*Wendt et al.*, 2008] and folding of sedimentary rocks [Vaughan et al., 2002a]. In the northern Antarctic Peninsula, the situation is less clear, although metamorphism of this age has been identified in the Scotia metamorphic complex [Trouw et al., 2000] and thrusting of volcanic rocks is evident in part of Graham Land [Vaughan, 1995]. Based on field relationships and direct dating, deformation is generally latest early Cretaceous in age. Radiometric dating control on the ages of structure formation and uplift suggests that deformation peaked in the interval 110–100 Ma [Leat et al., 2009; Storey et al., 1996; Vaughan et al., 1999, 2002a, 2002b]. The Palmer Land Event structural relationships described in this paper are developed in Eastern Domain sedimentary rocks and igneous rocks of the LCIS [Flowerdew et al., 2005; Vennum and Rowley, 1986] in Palmer Land.

### 3. The Eastern Domain and the Lassiter Coast Intrusive Suite

[13] The age of the underlying crust of the Eastern Domain comes from the Hf-isotope composition of inherited zircons in Paleozoic–Mesozoic granites, migmatites and paragneisses, which show that they are derived from Mesoproterozoic sources [Flowerdew et al., 2006]. The oldest rocks that crop out in the Eastern Domain terrane (Figure 1) are Late Mesoproterozoic metamorphic rocks at Haag Nunataks [Millar and Pankhurst, 1987; Wareham et al.,

1998] (Figure 1) and Paleozoic sedimentary rocks of the Fitzgerald Bluffs quartzite and Erewhon beds [Laudon and Ford, 1997]. These are overlain by Lower to Middle Jurassic silicic and basaltic volcanic rocks of the Ellsworth Land Volcanic Group [Hunter et al., 2006] (formerly the Mount Poster Formation [Riley and Leat, 1999; Rowley et al., 1983]), and basinal marine mudstones and shallow marine to terrestrial sandstones of the Middle Jurassic to earliest Cretaceous Latady Group [Hunter and Conrill, 2006] (formerly the Latady Formation [Rowley et al., 1983]). These host the LCIS [Vennum and Rowley, 1986] (Figure 2), a major complex of plutonic intrusions emplaced in southern Palmer Land over an area of  $800 \times 100$  km during the Early Cretaceous. Magmatic cooling ages fall in the interval 119–95 Ma, dated by Rb–Sr and K–Ar hornblende and biotite whole-rock–mineral isochron, and U–Pb zircon SIMS methods (Table S1 in the auxiliary material).<sup>1</sup> The suite ranges from acid to basic in composition, with a large proportion of intermediate composition calc-alkaline stocks and batholiths [Vennum and Rowley, 1986]. Rock types range from gabbro to granite, although granodiorite predominates. The suite consists of the Werner batholith, at  $225 \times 50$  km (Figure 2), and  $\sim 60$  smaller stocks and

<sup>1</sup>Auxiliary materials are available in the HTML. doi:10.1029/2011TC003006.

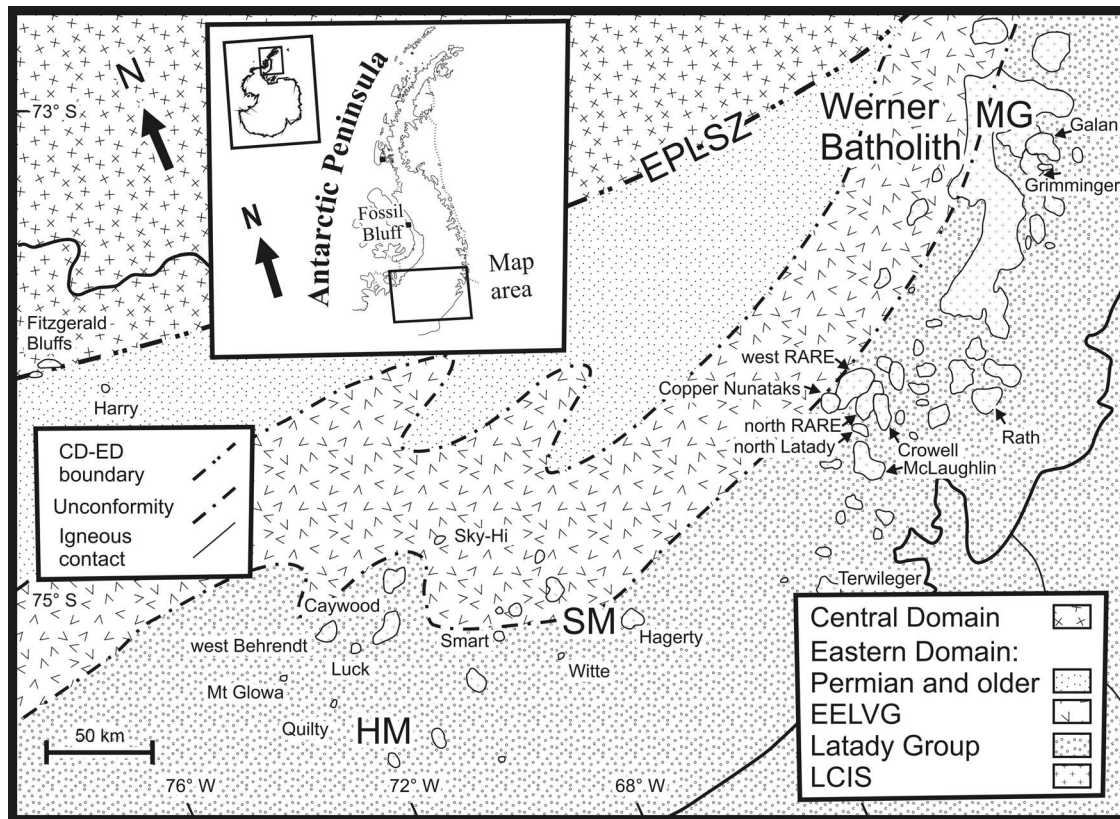


**Figure 2.** Interpreted geological map of the LCIS in largely ice-covered southern Palmer Land with names of dated plutons shown [after Pankhurst and Rowley, 1991]. EPLSZ, Eastern Palmer Land Shear Zone; EELVG, Eastern Ellsworth Land Volcanic Group; HM, Hauberg Mountains; LCIS, Lassiter Coast Intrusive Suite; MG, Mosby Glacier; and SM, Sweeney Mountains.

plutons, ranging from  $\sim 1$  km to  $\sim 20$  km across (Figure 2). Thermal aureoles are developed in the country rocks that are 1–2 km wide [Vennum and Rowley, 1986]. Metamorphic conditions reach hornblende-hornfels facies with minor migmatization of Jurassic rhyolites evident in some cases.

#### 4. Structural Data and Field Relationships

[14] Although a preliminary examination of the age data for the Palmer Land Event and the LCIS suggests that the Palmer Land Event occurred approximately mid-way through the interval of emplacement of the component plutons of the LCIS (110–100 Ma versus 119–95 Ma), apart from in northeast Palmer Land the relationships between plutonism and deformation, [Meneilly, 1983, 1988; Meneilly et al., 1987; Vaughan et al., 2002b], have not been examined in the field. Consequently, we examined the relative timing of deformation structures affecting components of the LCIS, and age-equivalent plutons north of the defined extent of the suite in eastern Palmer Land, and their country rocks. This was focused on seven areas of the Antarctic Peninsula (Table 1) along a distance of  $\sim 750$  km for which sufficient structural data exist (Figure 3). Three of the study areas, Mosby Glacier, Beaumont Glacier, and Mount Schimansky in the Welch Mountains (Figure 3), are new to the current study. Four of the study areas (Hauberg Mountains, Sweeney Mountains, Mosby Glacier and Beaumont Glacier; Table 1) are in the Eastern Domain and the remaining three (Mount

Jackson, Mount Shimansky and Mount Sullivan; Table 1) are in the Central Domain Eastern Zone. The structural data presented in Figure 3 are a compilation of published structural data collected by A.P.M. Vaughan, B.C. Storey and A.W. Meneilly [Meneilly, 1983, 1988; Meneilly et al., 1987; Vaughan and Storey, 2000] and new data collected by A.P.M. Vaughan during austral summer field seasons in 1999–2000 and 2003–04.

##### 4.1. Hauberg and Sweeney Mountains

[15] Latady Group [Hunter and Cantrill, 2006] rocks crop-out in the Hauberg Mountains and the southeastern part of the Sweeney Mountains. They consist of medium- to massive-bedded, rust weathering, quartz–feldspar wackes interbedded with thick laminated to very thin bedded siltstones in units up to 10 m thick. Rocks of the Latady Group are intercalated in their lower part with silicic and minor mafic volcanic rocks of the Eastern Ellsworth Land Volcanic Group (EELVG) [Hunter et al., 2006] which are developed in the northwestern part of the Sweeney Mountains (Table 1; labeled SM in Figure 2). Sedimentary and volcanic rocks are cut by the Hagerty and Smart plutons of the LCIS (Figure 2), as well as several smaller stocks. Structures are predominantly ductile to brittle-ductile with the development of meter- to 100 m-scale folding and penetrative cleavage in volcanic and sedimentary rocks, and spaced or fracture cleavage in plutonic rocks [Vaughan et al., 2002a]. Bedding is sub-horizontal to vertical or slightly overturned. Macroscopic folding is gentle

**Table 1.** Sample Localities Referred to in the Text

Locality Name	Centered On	Figured	Physiography	Terrane	Previously Studied?
Hauberg Mountains	75°50'S, 69°00'W	HM in Figures 2 and 3	A series of approximately north–south trending low topography ridges ranging from 1100 to 1300 m altitude	Eastern Domain	Yes [Vaughan <i>et al.</i> , 2002a]
Sweeney Mountains	75°07'S, 69°15'W	SM in Figures 2 and 3	East–west trending range of deeply dissected peaks, ranging from 1400 to 1700 m altitude.	Eastern Domain	Yes [Vaughan <i>et al.</i> , 2002a]
Mosby Glacier	73°00'S, 62°30'W	MG in Figures 2 and 3	Approximately 50 km long and 10 km wide, flowing NW–SE, into the New Bedford Inlet	Eastern Domain	No
Beaumont Glacier	72°30'S, 63°00'W	BG in Figures 3 and 6	Approximately 20 km long and 3 km wide flowing SW–NE from the Dyer Plateau to Hilton Inlet	Eastern Domain	No
Mount Jackson	71°24'S, 63°30'W	MJ in Figure 3	Series of ridges east and west of the main peak which is at 3184 m.	Central Domain	Yes [Vaughan and Storey, 2000]
Mt Schmansky (Welch Mtns)	70°47'S, 63°50'W	WM in Figures 3 and 8	series of discontinuous ridges that extend 10–12 km north and south from the main peak	Central Domain	No
Mount Sullivan	69°40'S, 63°47'W	MS in Figure 3	Series of arêtes and ridges extending northeast–southwest	Central Domain	Yes [Vaughan <i>et al.</i> , 2002b]

concentric to tight chevron and half-wavelengths are ~30–100 m. Folds plunge shallowly west-southwest, with steeply south-southeast dipping axial planes [Kellogg and Rowley, 1989]. Cleavage dips moderately to steeply, generally north-westward, fanning about fold axes [Kellogg and Rowley, 1989]. As previously described by Vaughan *et al.* [2002a], the granodiorite pluton at east Hagerty Peak and a microgranite dike at Bean Peaks, in the Hauberg Mountains to the south (Table 1; labeled HM in Figure 2), show structural and metamorphic relationships that suggest magma was emplaced after horizontal bedding rotation during folding but before development of the main regional cleavage. The age of these intrusive rocks, particularly the microgranite dike [Vaughan *et al.*, 2002a], indicates that formation of the main regional southwest-trending folding and cleavage occurred at ~107 Ma.

[16] As part of this study, the structural relationships were re-examined in the eastern part of Hagerty Peak (Hagerty in Figure 2; SM in Figure 3). The Hagerty Peaks pluton in the eastern part consists of rust-weathering, pale gray, fine- to medium-grained monzodiorite and quartz monzodiorite to granodiorite and granite [Rowley *et al.*, 1988]. It cuts steeply dipping quartzites and mudstones with intense thermal metamorphism and garnet skarn development. It was initially dated by Rowley *et al.* [1988] who analyzed hornblende and biotite by the K–Ar method, and interpreted concordant ages ranging from 112 to 116 Ma as the age of crystallization. The granodiorite was subsequently dated at ~113 Ma by Pankhurst and Rowley [1991], using the Rb–Sr whole rock method (Table S1).

[17] The regional cleavage is strongly developed in the granodiorite as a 1 to 10 cm-spaced anastomosing cleavage, mm-spaced in intense zones up to 50 cm wide, that strikes SW to WSW, and is continuous with cleavage in the hornfelsed Latady Group country rocks. The cleavage has been demonstrated to be parallel to cleavage in Latady Group rocks at Bean Peaks in the Hauberg Mountains (labeled HM in Figures 2 and 3) dated at ~107 Ma [Vaughan

*et al.*, 2002a]. Associated with this cleavage, a steep, WSW-striking, sinistral, bedding and cleavage parallel strike slip fault is developed cutting country rocks sediments with hornfels development.

[18] New data indicate that this approximately E–W cleavage is cut by a 2–5 cm spaced fracture cleavage/joint set at a high angle. This dips moderately to steeply east (Figure 3), and strikes approximately parallel to similar closely spaced joint sets developed in the Hauberg Mountains that cut WSW-striking penetrative cleavage in Latady Group rocks.

#### 4.2. Mosby Glacier

[19] As shown on the geology map (Figure 4), plutonic rocks of the LCIS form the bulk of the outcrop at Mosby Glacier (Table 1; labeled MG in Figure 3). To the east, the country rock consists of andalusite, hornblende or garnet bearing hornfels of sedimentary rocks with Latady Group affinities, and, to the west, stratigraphically older silicic volcanic rocks with EELVG affinities (Figure 4) with an inferred unconformable contact. In some cases, silicic volcanic rocks show evidence of small degrees of migmatite formation. Plutonic rocks range from diorite/gabbro and tonalite through to granite, with a predominance of granodiorite. Previous mapping [Vennum and Rowley, 1986] suggests that plutons are zoned, with mafic margins and felsic cores. Mafic enclaves are common and aplite/pegmatite dikes are abundant. Mafic, hornblende-phyric dikes cut the plutonic rocks in some few cases.

[20] New fieldwork has revealed that a steeply dipping, northeast-striking penetrative slaty to phyllitic cleavage is developed in the Latady Group country rocks (e.g., field station R.8256b; Figure 4). Cleavage development has overprinted aureole rocks forming augens of andalusite and garnet previously formed during thermal metamorphism. Ptygmatic and isoclinal folds associated with this deformation suggest that bedding may be transposed. Associated deformation appears to have folded late aplite/pegmatite

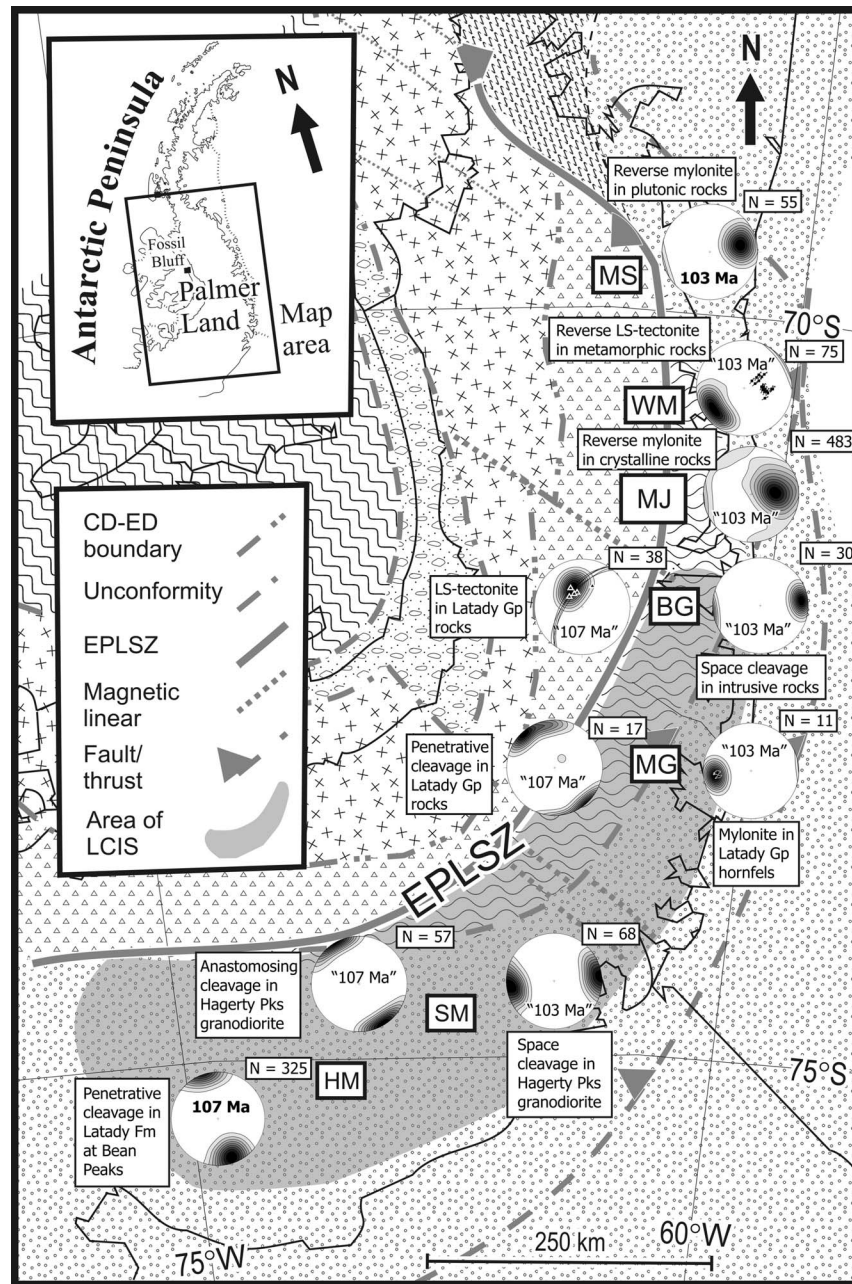


**Figure 3.** Map of Palmer Land depicting summary structural geological data for localities mentioned in the text and listed in Table 1. Abbreviations and shading as in Figure 1. Structural data are plotted on an equal-area lower hemisphere projection using Stereo32, version 1.0.3 [Röller and Trepmann, 2003]; and contoured using Fisher distribution and interpolation [Fisher et al., 1987]; and scaled to multiples of uniform distribution [Röller and Trepmann, 2003]. Lower hemisphere projections labeled “107 Ma” refer to older structures and labeled “103 Ma” refer to younger structures as explained in the text and summarized in Figure 9. Bold text indicates dated localities. Inset boxes with heavy borders show the areal extents of data collection localities and are labeled as follows: BG, Beaumont Glacier; HM, Hauberg Mountains; MG, Mosby Glacier; MJ, Mount Jackson; MS, Mount Sullivan; SM, Sweeney Mountains; WM, Welch Mountains. For Mosby Glacier, slip-linear plot [Hoepfener, 1955] of reverse shear tectonic lineations superimposed on contoured poles to mylonite foliation in Latady Group metasediment hornfels. For Beaumont Glacier, fold plunges, indicated by filled triangles, and fold axial planes, shown with great circles superimposed on contoured poles to plunge of L-S tectonite fabric in Latady Group rocks. For the Welch Mountains, slip-linear plot [Hoepfener, 1955] of reverse and dextral-reverse shear lineations on mylonite and blastomylonite fabric developed in gneissic granodiorite superimposed on contoured plunge directions for LS-tectonite developed in Mesozoic plutonic rocks at Mount Schimansky. EPLSZ is Eastern Palmer Land Shear Zone and LCIS is Lassiter Coast Intrusive Suite.

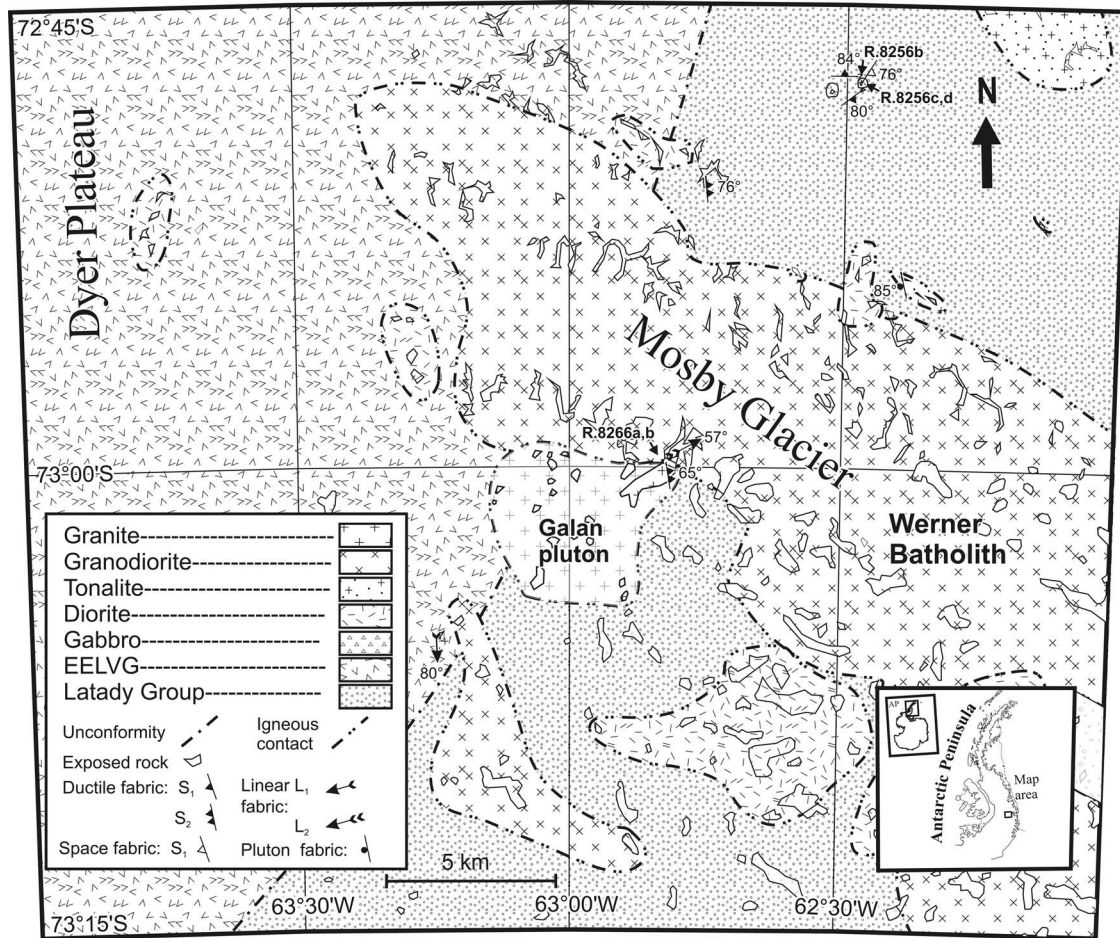


**Figure 4.** Summary geological map of the Mosby Glacier region. Visited field stations identified in bold type, e.g., R.8266a, b.

dikes in the main plutons. Spaced cleavages and jointing are evident in plutonic rocks, and similar to Hagerty Peak, the penetrative cleavage in the country rocks trends parallel to an intense spaced cleavage in diorite (e.g., field stations R.8256c,d; Figure 4).

[21] The penetrative cleavage is overprinted by a steeply east-northeast-dipping mylonitic foliation developed in andalusite hornfels metasediments of the Latady Group forming part of the aureole to the Galan pluton (Figures 2–4; field stations R.8266a,b). Thin section examination of microstructures in deformed hornfels (Figure 5) shows that pseudomorphs after andalusite form porphyroclasts with sigma and delta geometries [Passchier and Simpson, 1986] in ultramylonite. The sense of rotation of porphyroclast tails [Simpson and Depaor, 1993] indicates a reverse sense-of-shear. Andalusite pseudomorphs are replaced with sericite and epidote, although some relict fragments survive, showing the characteristic pink pleiochromism. Quartz pressure-shadows are evident on some grains extending out into porphyroclast tails.

[22] A mineral lineation is developed on mylonite surfaces plunging steeply northeast (R.8266a,b; Figure 4). The mylonite fabric shows increased shear strain over a width of 50 m to the pluton contact and is developed as ultramylonite adjacent to it. The granodioritic rocks in the vicinity of

the shear zone at the margin of the Galan pluton are also mylonitized with formation of ultramylonite. Dating of the Galan pluton by Farrar *et al.* [1982] using the K-Ar mineral method on biotite suggests that it cooled through the blocking temperature for Ar at  $104 \pm 3.8$  Ma (Table S1), which may either represent a magmatic cooling age, or the age of a resetting event associated with the reverse-shear mylonite deformation recorded in the aureole rocks.

#### 4.3. Beaumont Glacier

[23] The Beaumont Glacier (Table 1; labeled BG in Figure 3) sits at a broad transition between the rock associations of the Latady Group [Hunter and Cantrill, 2006; Rowley *et al.*, 1983] to the south, and those of the age equivalent Mount Hill Formation [Meneilly *et al.*, 1987; Storey *et al.*, 1987] to the north. Mount Hill Formation rocks are Jurassic to Cretaceous in age [Hunter and Cantrill, 2006; Vaughan and Storey, 2000] and it seems likely that these are in part equivalent to, but with higher intensity of deformation and grade of metamorphism, rocks of the Latady Group [Vaughan and Storey, 2000]. Additionally, the Beaumont Glacier marks the boundary between areas of differing character and feature-wavelength in aeromagnetic and aerogravity potential field data [Ferris *et al.*, 2002], possibly reflecting differences in crystalline basement rocks.

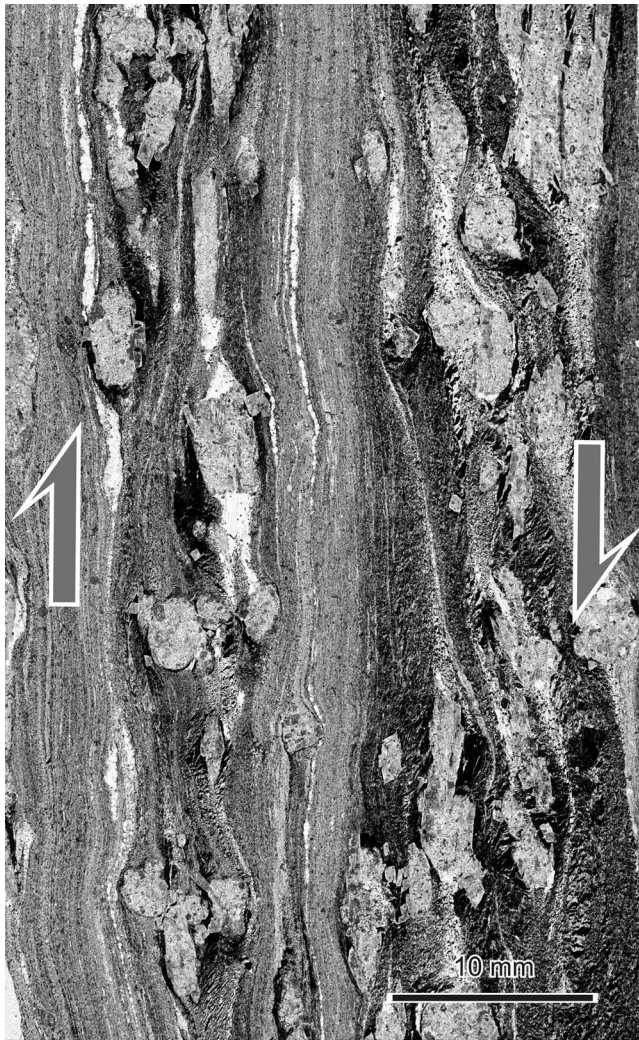


**Figure 5.** Photomicrograph of deformed Latady Group andalusite hornfels at Mosby Glacier (MG in Figure 3) showing andalusite pseudomorphs/relics, porphyroblast geometries and quartz pressure shadows. Half-arrows indicate sense-of-shear.

[24] Deformed metasedimentary rocks of the Latady Group crop are in possible unconformable contact with volcanic rocks of the EELVG (Figure 6). These are intruded by large granite, granodiorite and gabbro plutons that are the probable northward extent of the LCIS [Wever *et al.*, 1994]. High strain deformation of the EPLSZ is developed in the western part of the study area, and the shear zone forms the boundary with deformed crystalline rocks of the Central Domain to the west.

[25] Early and late deformation fabrics deform sedimentary and volcanic rocks, with relative ages determined from igneous intrusion crosscutting relationships. South of the Beaumont Glacier a steep, penetrative sub-mm-scale LS-tectonite plunging moderately west-northwest to northwest (BG, Figure 3;  $S_1$  and  $L_1$  in Figure 6) is developed in Latady Group and EELVG rocks. The LS-tectonite shows a mm-scale mineral stretching lineation defined by the long axes of andalusite porphyroblasts/porphyroclasts. Associated folding is developed and is most obvious in 2–20 cm thick microgranite

dikes cutting the metasilstone, although metasilstone fold closures are abundant (e.g., Figure 7). Folds are tight to isoclinal with thickening in the hinge zone. Half-wavelengths and amplitudes are on a dm- to m-scale. The main LS-foliation fans about fold axes and shows refraction across-folded units. Folds plunge steeply west-northwest to northwest and axial planes dip steeply northwest (BG, Figure 3).

[26] At field stations R.7629 and R.7630 (Figure 6), granodiorite sheets, andesite dikes, and pegmatite veins, marginal to a stock forming a previously unidentified component of the LCIS, crosscut the metasedimentary and metavolcanic rocks deformed by the LS-tectonite described above. In these igneous rocks, a mm-spaced anastomosing space cleavage is developed, dipping steeply to the west (Figure 3 and field station R.7630 in Figure 6). This is parallel to ductile SL- and L-tectonite reverse shear structures developed in Hjort Formation rocks in the main zone of the EPLSZ at field stations R.7622, 23 and 28 (Figure 6).

#### 4.4. Mount Jackson

[27] The structural geology at Mount Jackson (Table 1; labeled MJ in Figure 3) has been described by Vaughan and Storey [2000], who reported that in the vicinity of Mount Jackson, the EPLSZ is approximately 5 km across strike, with NW-striking zones of reverse and dextral-reverse mylonite. These are developed in K-feldspar megacrystic granite and gabbro and complex polymict breccias 30–80 m wide and 3 km along strike consisting of predominantly igneous lithologies, including acid to intermediate volcanic and tuffisitic rocks, granodiorite, gabbro, megacrystic and mylonitic granite, and appinitic rock, as well as clasts of reworked breccia composed of some or all of the preceding lithologies. No paragneissic rocks were observed. The breccia and mylonite zones form the boundary between metamorphic rocks and plutonic rocks of the Central Domain to the west, and probable Mesozoic metasedimentary and metavolcanic rocks of the Eastern Domain to the east similar to those described above from Beaumont Glacier. Megacrystic granite is deformed to protomylonite and mylonite in ductile reverse shear zones dipping west to west-southwest with a tectonic transport direction to the northeast.

#### 4.5. Welch Mountains, Mount Schimansky

[28] The Welch Mountains (Table 1; labeled WM in Figure 3) sit on the eastern edge of the Central Domain in the hanging wall of the EPLSZ, based on the interpretation of Vaughan and Storey [2000]. The range consists largely of paragneiss and orthogneiss cut by a sheared and foliated intermediate to mafic plutonic complex. LS-tectonite fabrics are common affecting metamorphic and plutonic rocks. Although radiometric ages from the range are sparse [Wever *et al.*, 1995], recent U-Pb zircon dating [Flowerdew *et al.*, 2006] indicates that the paragneissic rocks contain Neoproterozoic to Cambrian detrital zircons (~650–500 Ma). The ages of plutonic crystalline rocks in the Welch Mountains are unknown; however, the age of a leucocratic sheet intruding K-feldspar megacrystic granite and biotite orthogneiss from Mount Nordhill in the central part of the range [Flowerdew *et al.*, 2006] indicates that they are older than ~166 Ma (early Middle Jurassic). Porphyritic K-feldspar megacrystic granite similar to that from the Welch Mountains has been dated in the Central Domain Eastern Zone in northeast

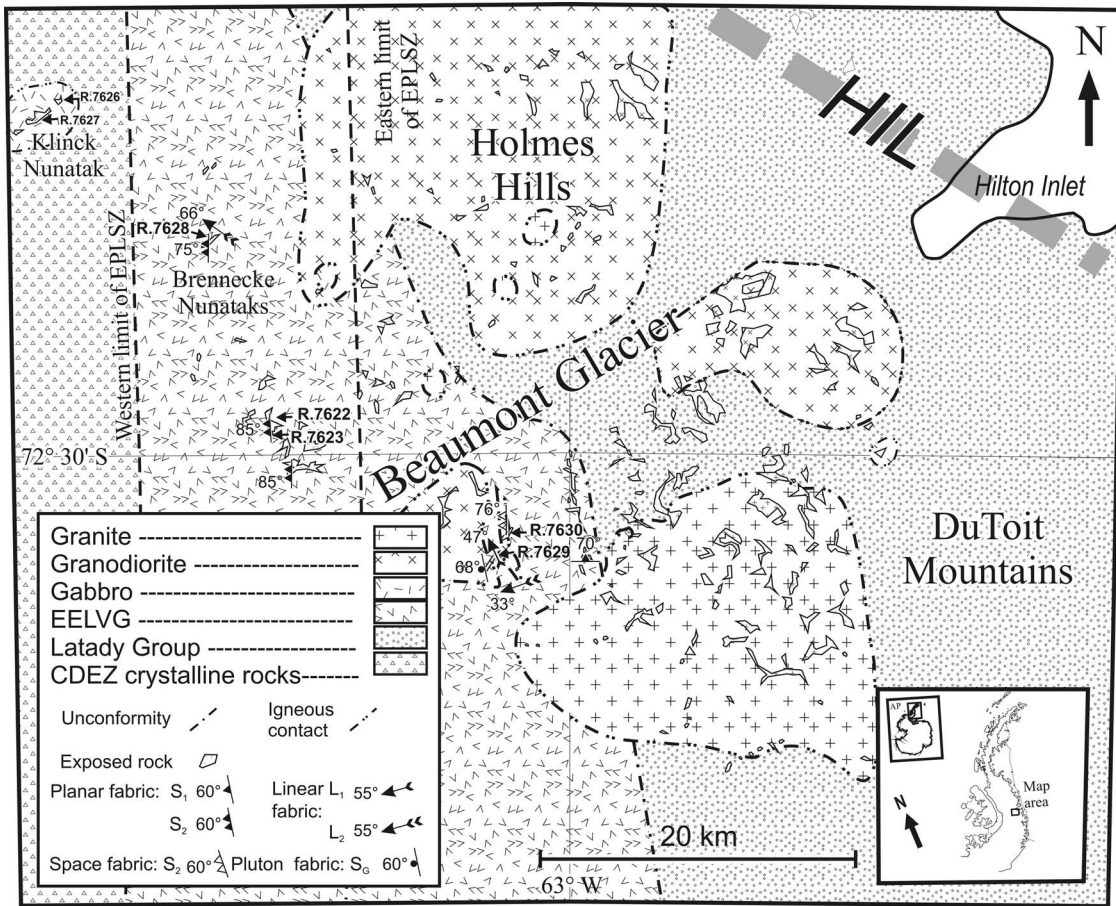


**Figure 6.** Summary geological map of the Beaumont Glacier region. Visited field stations identified in bold type, e.g., R.7629.



**Figure 7.** Profile view of folded Latady Group sandstones in the Du Toit mountains at field station R.7629 (Figure 6). Field notebook is 10 cm long.

Palmer Land at  $\sim 177$  Ma [Pankhurst, 1983] (latest Early Jurassic) and in the Central Domain Western Zone in western Palmer Land at  $\sim 260$  Ma [Millar *et al.*, 2002] (middle to late Permian).

[29] New data for the current study were collected in the northern part of the Welch Mountains at Mount Schimansky (Figure 8). The geology of the northern part of the Welch Mountains is dominated by a large granodiorite pluton centered on Liston Nunatak (Figure 8). This pluton is undated but it is deformed by Palmer Land Event LS-tectonite at field station R.7183 (Figure 8) and may be a component of the extended northward extent of the LCIS.

[30] The country rock is metamorphic. The northern ridge of Mount Schimansky consists of migmatized, blastomylonitic granodiorite gneiss with folded amphibolite dikes. Gneissic rocks have also been recorded southeast of the Liston Nunataks pluton but the affinity of this gneiss is unknown. It may form part of the paragneissic rocks that comprise the main part of the Welch Mountains. Smaller plutons intrude the country rock: a tonalite pluton forms the main part of Mount Schimansky and gabbro was mapped in the northern part of the study area (Figure 8).

[31] Deformation structures at Mount Schimansky are dominated by high strain northeast-directed ductile structures associated with the main phase of the Palmer Land Event; however, at field station R.7173 (Figure 8) a nebulitic gneiss foliation representing a relict early fabric dips moderately northwest, strike-parallel with early phase structures seen farther south.

[32] The blastomylonitic granodiorite gneiss fabric consists of a partially recrystallized shallowly west- to southwest-dipping domainal SL-tectonite ( $S_2$  in Figure 8) defined by planar assemblages of hornblende and biotite. The fabric has a reverse to reverse-dextral sense-of-shear from  $\sigma$ -porphyroblast indicators (WM in Figure 3). Slip-linear representation of the data (WM in Figure 3) shows a consistent tectonic transport direction to the northeast. Plutonic rocks show grain boundary and enclave defined magmatic fabrics that dip moderately southwest in tonalite and steeply north in granodiorite ( $S_G$  in Figure 8; R.7179). Gabbro and granodiorite are penetratively deformed by an L- and LS-tectonite fabric with a lineation that plunges shallowly to the southwest (WM in Figure 3 and  $L_2$  in Figure 8; R.7183) and parallel to the tectonic transport direction determined for the blastomylonitic fabric. The L- or LS-tectonite fabric is defined by a strong alignment of grain-long-axes of feldspar or hornblende, depending on rock composition, and grain boundaries of hornblende and biotite or chlorite. Flattened, prolate xenoliths of microdiorite and microgranodiorite also have long-axes aligned parallel to the granodiorite L-fabric in zones of high strain.

#### 4.6. Mount Sullivan

[33] Mount Sullivan (Table 1; labeled MS in Figure 3) consists of crystalline metamorphic rocks include layered, quartzofeldspathic gneiss, mafic, garnetiferous restitic gneiss, and migmatite. Plutonic rocks are commonly highly deformed, but include, gabbro, porphyritic diorite, porphyritic granodiorite dated at  $\sim 177$  Ma [Pankhurst, 1983], and Triassic granite (I. Millar, BAS unpublished data, 1999). The EPLSZ at Mount Sullivan was described in detail by Vaughan *et al.* [2002b]. It forms a high-strain, ductile zone that deformed crystalline,

metamorphic rocks, gabbroic to granitic plutons and metasedimentary rocks [e.g., Meneilly, 1988] and dips steeply west with an overthrust sense to the northeast (MS in Figure 3). Deformation ranges from proto- to ultramylonite and pseudotachylyte, with major zones of breccia developed to the east [Meneilly, 1988]. Vaughan *et al.* [2002b] dated reverse shear in Jurassic gabbro from the main zone of the EPLSZ at Mount Sullivan at  $\sim 103$  Ma.

## 5. Interpretation

### 5.1. Relative Timing of Deformation

[34] In the Eastern Domain localities at the Hauberg Mountains, Sweeney Mountains, Mosby Glacier, and Beaumont Glacier, structures trending approximately east-northeast–west-southwest are cut by planar structures trending north-northwest–south-southeast, or by L-tectonite structures plunging to west-southwest. Qualitatively, and away from the immediate thermal effects of pluton emplacement as seen at Mosby Glacier, earlier ductile to brittle-ductile structures, in some cases associated with sinistral shear (such as at Hagerty Peak; labeled SM in Figure 3), are deformed by later brittle-ductile structures, possibly suggesting relative exhumation of the earlier structures before development of the later; however, this has not been quantified. Overall, a consistent tectonic overprinting relationship is evident in southern Palmer Land.

[35] In the Central Domain Eastern Zone localities from Mount Schimansky northward, this overprinting relationship is not developed. No earlier fabric is observed there (WM in Figure 3) although the relative orientation of reverse-shear lineations on the blastomylonitic fabric suggests that this may be a reactivated earlier foliation. At Mount Jackson (MJ in Figure 3) the lower hemisphere plot of contoured poles to reverse shears shows a distribution pattern that is consistent with elements of both earlier and later structures being present, although later structures are dominant and no attempt to age-discriminate between structures was made as part of this study. It is notable that Beaumont Glacier is the northernmost area where a clear overprinting relationship is observed. Beaumont Glacier has been identified from geophysical data as marking a significant crustal boundary in the eastern Antarctic Peninsula [Ferris *et al.*, 2002] associated with Gondwana break-up. The current study indicates that it marks a change in intensity of development of later deformation fabrics, with more intense and ductile expression of these fabrics north of Beaumont Glacier.

[36] Later structures see their fullest flowering in the EPLSZ [Vaughan and Storey, 2000], which strikes approximately N-S in eastern Palmer Land and is pervasively developed as a ductile mylonitic shear zone with reverse and dextral-reverse sense of offset and tectonic transport direction to the northeast. For example, the mean plunge of the tectonic fabric at Mount Sullivan is  $58^\circ$  to  $248^\circ$  [Vaughan *et al.*, 2002b], is largely parallel to the trends observed for the later fabrics described above. The later structures contain a higher proportion of LS-, L- and SL-tectonites than those of the earlier deformation, consistent with a qualitative assessment of higher observed strain for the EPLSZ and possibly indicating higher temperatures during deformation. Tectonites with predominantly L-geometries [Flinn, 1965] may indicate deformation under a transtensional strain regime, as has been

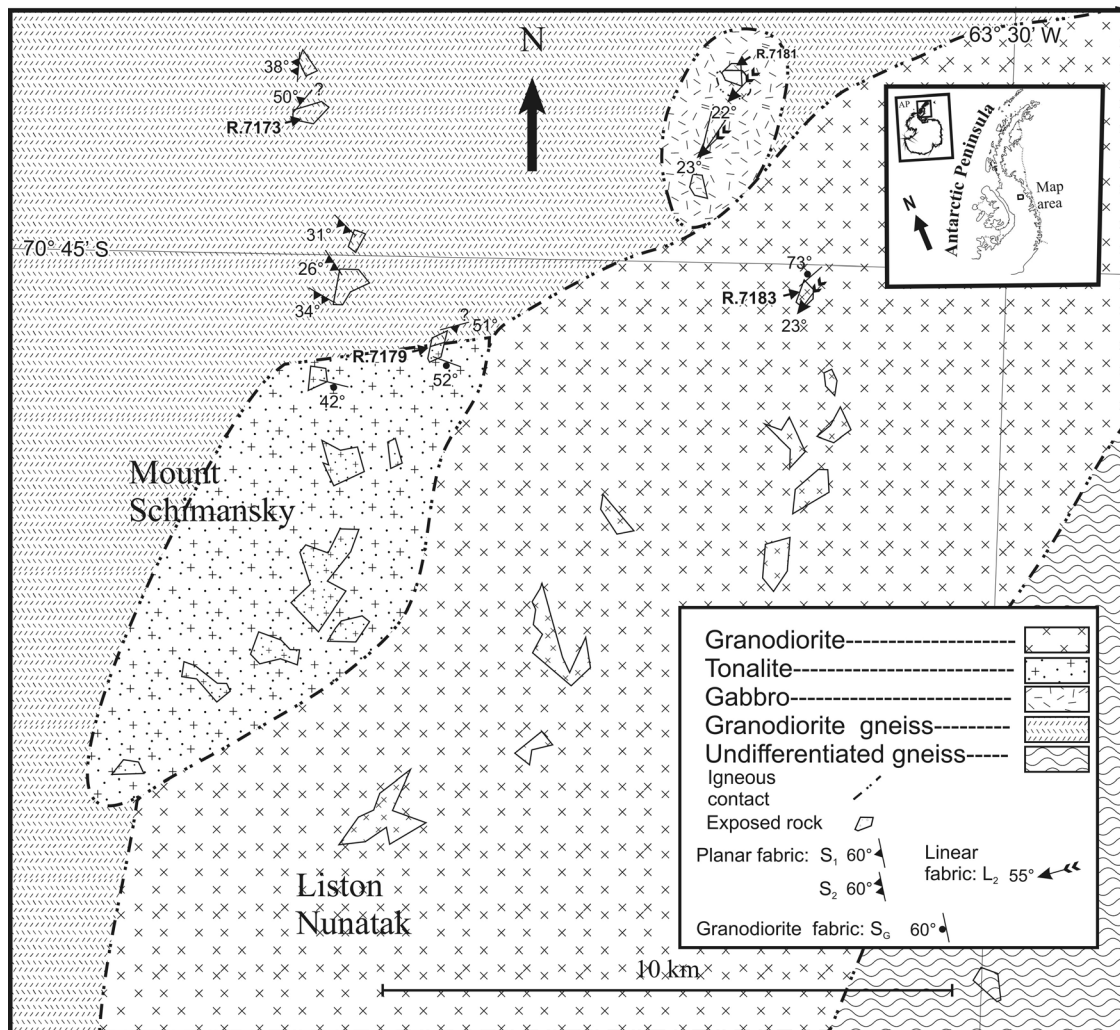


**Figure 8.** Summary geological map of the Mount Schimansky area. Visited field stations identified in bold type, e.g., R.7183.

suggested for Marie Byrd Land [McFadden *et al.*, 2010], possibly hinting at extensional episodes during the Palmer Land Event.

## 5.2. Two Separate Phases for the Palmer Land Event

[37] Figure 9 shows summary contoured lower hemisphere equal area plots that compile all structural data that can be attributed to the two phases of the Palmer Land Event along approximately 750 km of the southern Antarctic Peninsula. Data plotted in Figure 9 includes new structural data presented above and structural data from Ellsworth Land and Palmer Land published by Vaughan *et al.* [2002a, 2002b] and Vaughan and Storey [2000]. Figure 9a is a compilation of the structures plotted on lower hemisphere equal area plots labeled “107 Ma” in Figure 3; Figure 9b is a compilation of the structures plotted on lower hemisphere equal area plots labeled “103 Ma” in Figure 3. The data show that structures from the earlier phase of the Palmer Land Event (Phase 1, Figure 9a) have a mean dip azimuth of  $341^\circ$  ( $n = 380$ ), averaging a paleostrain direction which can be equated with the orientation of the principal compressive stress at the time of deformation. Similarly, structures from

the later phase of the Palmer Land Event (Phase 2, Figure 9b) have a mean dip azimuth of  $259.5^\circ$  ( $n = 747$ ), averaging a paleostrain direction that reflects the subsequent principal compressive stress direction. The most recent paleomagnetic data for the southern Antarctic Peninsula indicate that the region was in or near to its present-day position with respect to East Antarctica by  $\sim 130$  Ma and has not undergone significant rotation or horizontal translation relative to East Antarctica since  $\sim 110$  Ma [Grunow, 1993]. This assessment places some confidence that mid-Cretaceous paleostain directions have been preserved and are reliable for evaluation of models of Cretaceous plate kinematics.

## 5.3. Absolute Age Control

[38] Fortunately, existing age data for Palmer Land Event deformation structures in the eastern Antarctic Peninsula record the ages of representative structures trending parallel to the Phase 1 and Phase 2 orientations outlined above, allowing quantitative timing constraints to be placed on the evolution of deformation. As referred to above for the Hauberg Mountains, Vaughan *et al.* [2002a] showed that a felsic dike, associated with the LCIS, that cuts Latady Group

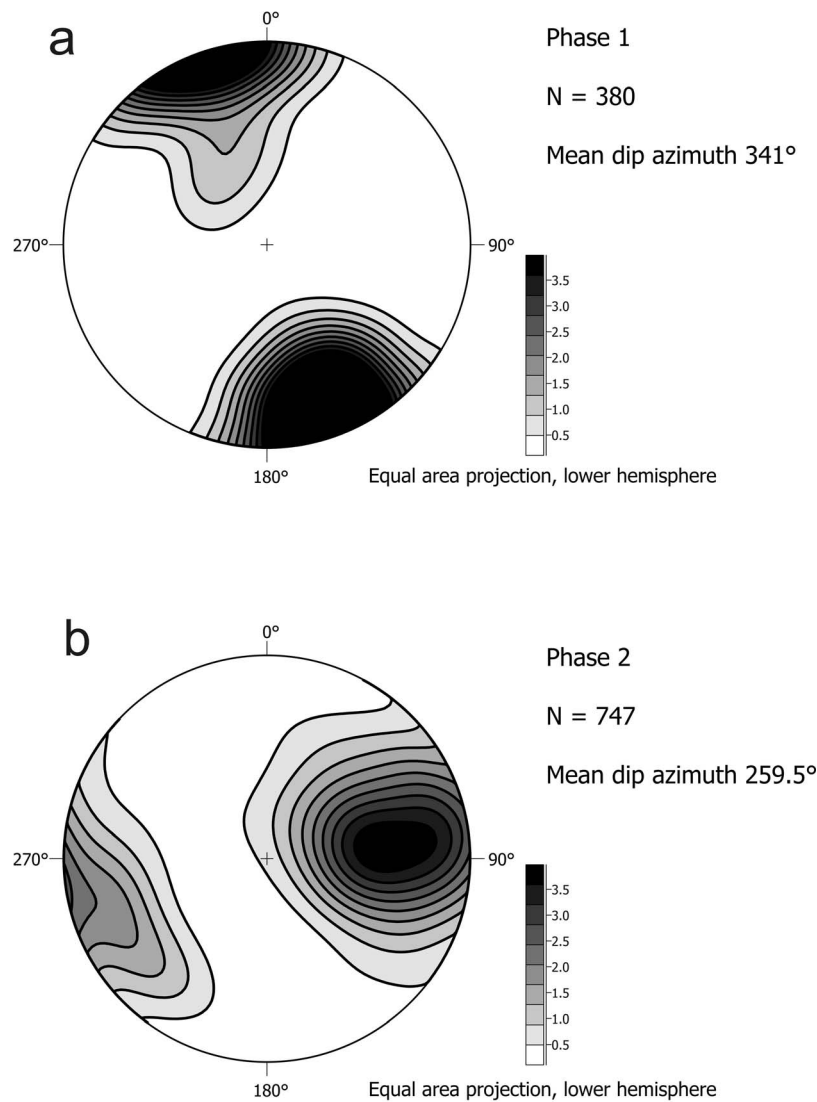


**Figure 9.** (a) Contoured compilation of Palmer Land Event structures from lower hemisphere projections labeled “107 Ma” in Figure 3, identified as “early” using criteria described in the text. (b) Contoured compilation of Palmer Land Event structures from lower hemisphere projections labeled “103 Ma” in Figure 3, identified as “late” using criteria described in the text. Plots are compilations of data incorporating poles to planar fabrics and plunges of linear fabrics. Structural data are plotted on an equal-area lower hemisphere projection using Stereo32, version 1.0.3 [Röller and Trepmann, 2003]; contoured using Fisher distribution and interpolation [Fisher *et al.*, 1987]; and scaled to multiples of uniform distribution [Röller and Trepmann, 2003].

sandstones overlapped Phase 1 cleavage development on the basis of structural relationships. They dated the dike, and, by association, a time of active cleavage formation in Latady Group rocks, at  $106.9 \pm 1.1$  Ma by uranium-lead SIMS method dating on zircon. The penetrative cleavage in the Latady Formation rocks and in the felsic intrusion dips steeply north-northwest and is parallel to the early Palmer Land Event structures described above. At the northern end of the EPLSZ, biotite from Jurassic gabbro at Mount Sullivan mylonitized during Phase 2 has been dated at  $102.8 \pm 3.3$  Ma [Vaughan *et al.*, 2002b] by Ar-Ar laser method dating. Mount Sullivan shows intense development

of reverse-dextral mylonite of the EPLSZ dipping moderately west-southwest, trending parallel to the Phase 2 planar structures described above and with a tectonic transport direction parallel to later Palmer Land Event L-tectonites.

#### 5.4. Relationship to LCIS Emplacement

[39] The age data described above indicate that both phases of the Palmer Land Event in southern and eastern Palmer Land overlap with the main phase of emplacement of the LCIS; however, more detailed analysis is possible. To this end, a data set of 42 LCIS emplacement ages (Table S1) was compiled. These consist of magmatic cooling ages derived

using a variety of Rb-Sr and K-Ar methods (Table S1) and crystallization ages obtained by U-Pb SIMS zircon dating. The data set only includes mineral ages that are considered reliable. For Rb-Sr biotite ages this means determinations with  $^{87}\text{Rb}/^{86}\text{Sr}$  ratios  $>90$  are included and for K-Ar ages only analyses with measured K contents ( $>6\%$  for biotite,  $>0.6\%$  for hornblende) and measured radiogenic Ar ( $>80\%$ ) are included. These measures are considered to identify and remove analyses which have experienced post-crystallization perturbations and which lead to erroneous ages. Rb-Sr whole rock ages are also excluded on their basis of their possible erroneous age determinations [Flowerdew *et al.*, 2005]. A cumulative frequency plot of these LCIS age data and age data for the two deformation phases of the Palmer Land Event shows detailed timing relationships (Figure 10).

[40] As shown in Figure 10, the Phase 1 of the Palmer Land Event appears to have coincided with a major peak in intrusion rate for components of the LCIS [Flowerdew *et al.*, 2005; Vennum and Rowley, 1986], whereas Phase 2 does not, and may coincide with a lull. The timing relationships suggest that paleostress changes associated with Phase 1 of the Palmer Land Event may have enhanced the intrusion rate of the plutonic suite, although there is insufficient information to identify these in detail.

### 5.5. Possible Kinematic Control on LCIS Emplacement

[41] A recent synthesis [de Saint Blanquat *et al.*, 2011] suggests that there is a relationship between pluton size and the ability of plutons to record regional deformation. Small plutons (less than 300 cubic kilometers in volume) are emplaced rapidly, in less than 100,000 years, via a series of magma pulses and are likely to record deformation only associated with magmatic emplacement. Larger plutons (up to 12,000 cubic kilometers) are also formed by magma pulses, but the duration of pluton formation, up to 10 million years, means that they grow on timescales likely to preserve evidence of regional deformation. The rate of magma pulse formation is primarily controlled by tectonics [de Saint Blanquat *et al.*, 2011], and therefore tectonic setting and processes determine the ultimate total volume of a particular plutonic complex or suite. A very cursory examination of the LCIS in map view (Figure 2) shows that many of the plutons are circular or close to circular in plan, indicating relatively rapid growth. Only the Werner batholith deviates from this planform suggesting that it may have grown on a million-year timescale, consistent with geochronological evidence for multistage development of the batholith [Pankhurst and Rowley, 1991], and have preserved evidence of regional deformation during its growth. It has a complex shape in plan view but interpretation of structural or tectonic implications are out with the present study. The interpreted kinematics associated with Phase 1 of the Palmer Land Event are consistent with studies that show preferential emplacement of plutons during transpression deformation [Glazner, 1991; Sharp *et al.*, 2000]. The timing relationships with deformation suggest that the magma generation or transfer rate associated with any subduction-related plutonism forming the suite was enhanced by Phase 1 of the Palmer Land Event and possibly inhibited by Phase 2, although examination of age-related compositional and isotopic variation in the LCIS, and detailed examination of pluton field relationships, would be needed to test this hypothesis.

### 5.6. Inferred Palmer Land Event Paleostains and Kinematics

[42] Figure 11 shows the inferred paleostain directions on a terrane map of the Antarctic Peninsula, with a likely kinematic interpretation for the two episodes of Palmer Land Event deformation based on the relationship to mega-structures observed in the field. Phase 1 of the Palmer Land Event appears to represent an episode of north-northwest–south-southeast shortening with a component of sinistral transpression depending on the orientation of major structures onshore. This phase is largely developed in the Eastern Domain in southern Palmer Land and is completely overprinted by Phase 2 north of Mount Jackson. The later and more intensely developed Phase 2 is associated with a west-southwest–east-northeast shortening direction and formation of the EPLSZ. It is developed as dextral transpression in the Eastern Domain in the southwest Antarctic Peninsula, but orthogonal compression in the Central Domain in northeast Palmer Land where the maximum development of the EPLSZ is seen [Vaughan and Storey, 2000]. This deformation phase is mainly developed between  $68^{\circ}\text{S}$  and  $74^{\circ}\text{S}$  (Figure 11) affecting central and northern Palmer Land and Alexander Island, but is only weakly developed in southern Palmer Land and Graham Land.

### 5.7. Relationship to Offshore Plate Kinematics

[43] The igneous geochemistry of the composite Central Domain terrane has been characterized as primitive in Palmer Land [Ferraccioli *et al.*, 2006; Wareham *et al.*, 1997], suggesting partial melting of intraoceanic mantle that is most simply reconciled with an intraPacific origin. On the other hand, there is a body of evidence that northern Graham Land and the Eastern Domain of Palmer Land share a pre-Cretaceous history with Andean Patagonia in terms of common provenance of Mesozoic sedimentary rocks, similarities of pre-Mesozoic metamorphic basement and the presence of now-separated parts of a Jurassic silicic igneous province [Barbeau *et al.*, 2010; Bradshaw *et al.*, 2012; Hervé *et al.*, 2006; Riley *et al.*, 2010]. To understand terrane amalgamation events involving the EPLSZ, therefore, it is necessary to understand the Cretaceous plate kinematics of East Antarctica, South America, and the intraPacific plates that subducted beneath them. This task is specifically challenged by the loss of Pacific Cretaceous seafloor to subduction, and by the timing of the Palmer Land Event well within the Cretaceous normal polarity superchron (124–84 Ma), through which no useful magnetic isochron data exist.

[44] In the Pacific Ocean, the plate kinematic history recorded in the surviving tracts of mid-Cretaceous seafloor, to the east of the Hikurangi-Tonga trench, is still being deciphered. It seems clear that this seafloor formed by the divergence of the oceanic Pacific and Phoenix plates from each other and at least one further plate, but interpretations of this plate's identity and kinematics differ. One of these interpretations, Sutherland and Hollis's [2001] Moa Plate, is suggested to have suffered dextral-oblique convergence and subduction along the entire West Antarctic margin, consistent with structural indications for the emplacement of the Western and Central domains in accompaniment to dextral transpression [Vaughan and Storey, 2000]. Other interpretations of the third plate [Eagles *et al.*, 2004; Larson

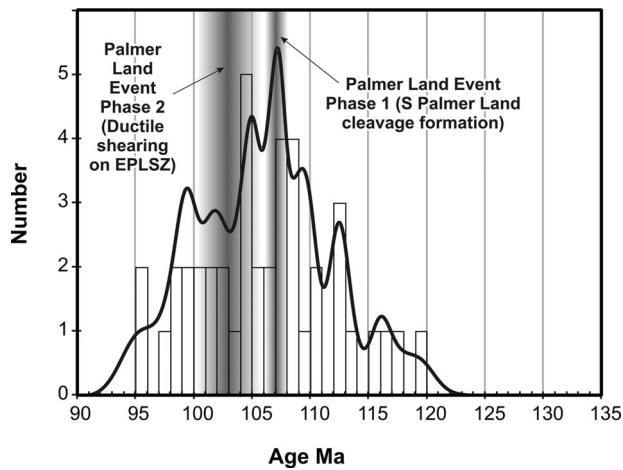


**Figure 10.** Cumulative frequency diagram [Ludwig, 2003] of ages for the LCIS (heavy black line and histogram), from Table S1, plotted against deformation ages (gray columns) determined for structures associated with the two phases of the Palmer Land Event. Deformation ages are based on published data and columns have been subjected to a Gaussian blur that reflects the two-sigma error on the radiometric data.

*et al.*, 2002; *Larter et al.*, 2002; *Worthington et al.*, 2006], while disagreeing on its size and location, all conclude that it did not influence much or any of the Palmer Land sector of the Antarctic margin, where subduction of the Phoenix plate

was occurring at the time of the Palmer Land Event (Figure 12b). Calculating the convergence direction between the Phoenix and Antarctic plates at this time with accuracy is not an easy task, as those plates were not linked by a circuit of divergent boundaries. This necessitates the use of a global hot spot reference frame with demonstrable, but unquantified, imperfections. Nonetheless, by assuming only slow relative motions between Pacific and Indo-Atlantic hot spots in Cretaceous times, the following statements allow a coarse picture of Phoenix-Antarctic relative motion to be drawn (Figure 12a).

[45] 1. Southern parts of the Pacific plate were moving at  $\sim 3.5$  cm/yr, toward the northwest in a Pacific hot spot reference frame, in the period 100–80 Ma [e.g., *Koppers et al.*, 1998]. There are no large changes in the Pacific apparent paleomagnetic wander path in the preceding 10 Myr [Sager, 2006], so that similar directions and rates can be envisaged for the time of the Palmer Land Event.

[46] 2. Tectonic flowlines and abyssal hill fabric [Larson *et al.*, 2002] preserved in a long ( $\sim 3600$  km) strip of Cretaceous normal polarity superchron crust to the east of the Hikurangi-Tonga Trench show that the Phoenix plate moved rapidly ( $\sim 20$  cm/Myr) toward the south-southeast with respect to the Pacific plate at the same time. Assuming this motion occurred about a distant Euler axis, southern parts of the Phoenix plate can also be assumed to have been moving toward the south-southeast with respect to the Pacific plate.

[47] 3. The Eastern Domain, as part of East Antarctica, was rotating in an Indo-Atlantic hot spot reference frame

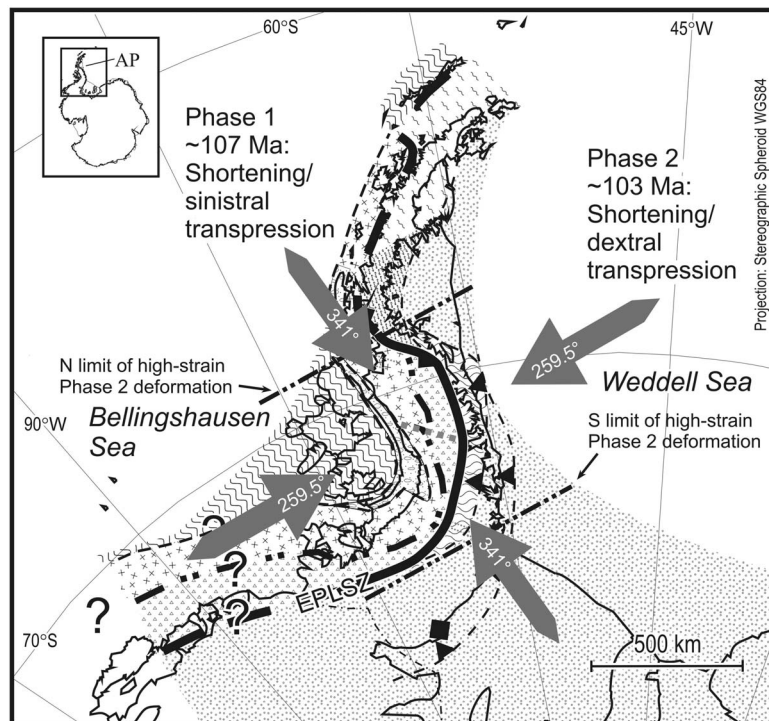


**Figure 11.** Measured paleostrain directions for Phase 1 (107 Ma) and Phase 2 (103 Ma) of the Palmer Land Event, from Figure 9, shown on the terrane map of the Antarctic Peninsula from Figure 1, with a likely local kinematic interpretation for the two episodes of deformation based on the relationship to megastructures observed in the field. Heavy double-dot-dashed lines indicate southern and northern limits of the maximum strain zone for Phase 2. Symbols and ornament as for Figure 1. EPLSZ is Eastern Palmer Land Shear Zone.

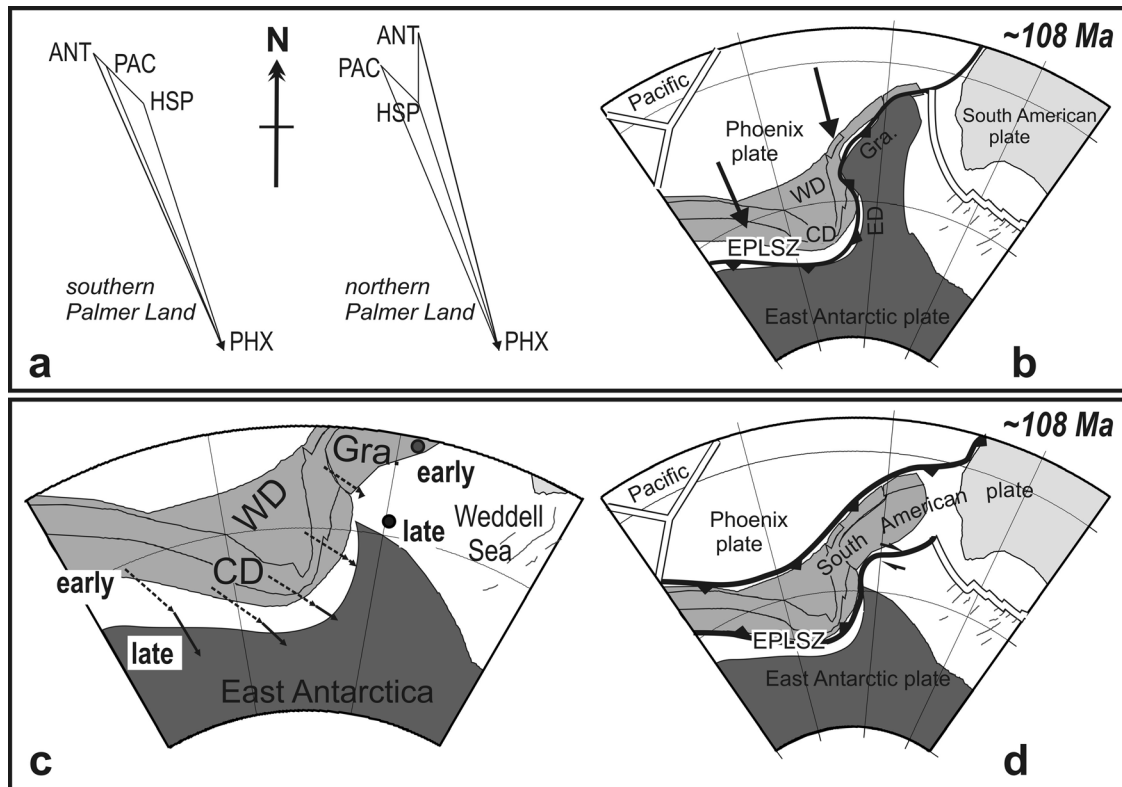


**Figure 12.** (a) Velocity triangles for Phoenix–Antarctic plate convergence in southern and northern Palmer Land (all hot spots assumed to be stationary in the mantle). (b) Plate tectonic setting of collisions involving Eastern Domain (ED) and Graham Land (Gra.) as part of the East Antarctic plate and Western and Central domains (WD and CD) within the Phoenix Plate. (c) Predicted flow lines for South American–Antarctic plate convergence along the EPLSZ. Dots indicate Euler poles for South American–East Antarctic motion through ‘early’ and ‘late’ parts of the Cretaceous normal polarity superchron. Dashed and whole arrows are flow line segments associated with rotation of points on the South American plate about these poles. Thin lines are fracture zones in the Weddell Sea. (d) Plate tectonic setting of collisions involving Eastern Domain as part of the East Antarctic plate and Western Domain, Central Domain and Graham Land moving with the South American plate. EPLSZ marks boundary that will develop into the Eastern Palmer Land Shear Zone.

such that its northern parts moved toward the northwest at  $\sim 5$  cm/Myr, and its southern parts moved at a similar rate toward the north [Müller *et al.*, 1993].

[48] The resultants by summation of these vectors for Phoenix–Antarctic convergent motion are dominated by the magnitude of the Pacific–Phoenix relative motion vector and suggest, regardless of the position along the EPLSZ, that the Phoenix plate converged with the East Antarctic plate along an azimuth a few degrees either side of SSE ( $337.5^\circ$ ; Figure 12b). Within the uncertainties mentioned above, and in the structural measurements, this is fully consistent with the  $341^\circ$  orthogonal shortening estimate from structural studies of the Palmer Land Event described above.

[49] The relative plate motions of East Antarctica and South America during the Cretaceous normal polarity superchron are reasonably well understood, albeit still at low resolution. Eagles and Vaughan [2009] were able to derive Euler rotations for these plates by modeling fracture zone orientations through the narrow strip of Weddell Seafloor built during the superchron. In the Weddell Sea itself, these fracture zones betray a continual change from northeast–southwest,

via north–south, to northwest–southeast divergence. The two stage poles describing this divergence are situated within Palmer Land, and thus imply convergence between the Eastern Domain and terranes farther west that were fixed to the South American plate (Figure 12c). The azimuth of this convergence changes along the EPLSZ in the range between SE and SSE ( $315$ – $337.5^\circ$ ; Figure 12d). This too is consistent with the structural indications for convergence along  $341^\circ$  during the 107 Ma Phase 1 of the Palmer Land Event, but requires northwest-directed subduction along the eastern margin of the Central Domain (Figure 12d).

## 6. Discussion

### 6.1. Implications for Models of Oroclinal Bending

[50] Oroclines, curved mountain belts, have attracted scientific interest since at least the 1920s [e.g., Argand, 1924] and the origin of curvature has been explained by three hypotheses [e.g., Yeh and Bell, 2004]: (1) original shape of the plate boundary; (2) vertical axis rotation during orogenesis, so-called bending, and; (3) overprinting of

orogenic events of different ages. The curvature of the Antarctic Peninsula has been noted since the 1960s [Hamilton, 1967], and early paleomagnetic studies [Kellogg, 1980] suggested that the curvature of the southern Antarctic Peninsula may have been related to oroclinal bending, i.e., differential vertical axis rotation during a single orogenic phase. Subsequent, more comprehensive, paleomagnetic analysis did not support a model of vertical axis rotation [Grunow, 1993]; however, this was not evaluated using structural geological data. The structural data presented above show superposition of Phase 2 Palmer Land Event structures on Phase 1 structures with a high angle of intersection (almost 90°), and geochronological data indicate a time gap of several million years between the end of development of Phase 1 structures and the short-lived pulse of deformation associated with Phase 2. Apart from at Mount Jackson or Beaumont Glacier there is little evidence for vertical axis rotation of earlier structures by Phase 2. By analogy with studies of the Ordovician Kingston orocline in North America [Marshak and Tabor, 1989], this provides strong evidence that the change in trend between southern and eastern Palmer Land is an intersection orocline produced by the superposition of Phase 2 on Phase 1 structures, creating an apparent bend on the spine of the Antarctic Peninsula of approximately 90°. The new evidence here indicates that vertical axis rotation, so-called oroclinal bending, is unlikely to be the source of the Antarctic Peninsula curvature in Palmer Land.

### 6.2. Phase 1 Regional Correlations

[51] Examination of kinematic interpretations along the Gondwana margin regionally in the Antarctic Peninsula and Chile show that Jurassic and Cretaceous rocks preserve structural evidence of sinistral shear or sinistral transpression resulting from compression prior to 100 Ma along an approximately NW–SE paleostain axis comparable to that inferred for Phase 1. On Alexander Island, subduction complex rocks of the LeMay Group show evidence of southeast-directed subduction-related convergence with sinistral transpression from middle Jurassic to early Cretaceous times [Doubleday and Storey, 1998]. In the Northern Antarctic Peninsula, structural analysis of early Cretaceous fault patterns developed in the Upper Jurassic Nordenskjöld Formation of the Trinity Peninsula indicate a NW–SE paleostain axis producing sinistral transpression [Vaughan and Storey, 1997; Whitham and Storey, 1989]. Cretaceous subduction complex rocks on Elephant Island in the South Shetland Islands of the northern Antarctic Peninsula preserve evidence of sinistral transpression developed during NNW–SSE-southeast compression prior to 100 Ma [Trouw et al., 2000]. East of the Antarctic Peninsula, seismic data indicate WNW–ESE compression producing sinistral transpression along 70 km of the southern Palmer Land–Weddell Sea margin affecting middle Jurassic to early Cretaceous rocks of the Latady Group [King and Bell, 1996]. In southern Chile, the Liquine-Ofqui fault zone preserves evidence of a sinistral transpression phase that predates 100 Ma granitic rocks [Cembrano et al., 2000]. Overall, inferred Mesozoic oceanic plate convergence with accretionary complexes on the Paleo Pacific margin of southern South America indicate left lateral convergence and sinistral shear [Hervé et al., 2006; Hervé et al., 2008; Poblete et al., 2011]. Recognition of Cretaceous deformation of this

style in the Antarctic Peninsula helps reconcile its strain kinematics with those of the Mesozoic paleo-Pacific coast of southern South America [Hervé et al., 2006].

### 6.3. Phase 2 Regional Correlations

[52] Phase 2 of the Palmer Land Event is more enigmatic and regional evidence of comparable structures is less abundant, although there is evidence of significant tectonism coeval with it. For example, on Alexander Island, cessation of deposition of the Fossil Bluff Group forearc basin and exhumation of its rocks occurred at approximately 100 Ma [Storey et al., 1996] and LeMay Group subduction complex rocks show evidence of a second phase of compressive deformation, overprinting the structures associated with Phase 1, with structures formed by southwest–northeast tectonic transport and dextral transpression [Doubleday and Storey, 1998]. Unconformities of this age are present in northwest Palmer Land [Leat et al., 2009]. There is some evidence for deformation of this age north of the Antarctic Peninsula. For example, in central Chile, Lower Cretaceous volcanic rocks were deformed by east–west compression associated with dextral transpression along the Silla del Gobernador shear zone between 109 Ma and 100 Ma [Arancibia, 2004]. The structural and geochronological evidence presented above would suggest that Phase 2 of the Palmer Land Event was short-lived and intense and resulted in the highest strain development of the EPLSZ. Significantly, the end of Phase 2 marks the termination of compressional deformation in the southern Antarctic Peninsula: subsequent Late Cretaceous tectonism is transtensional [Scarrows et al., 1997; Storey and Nell, 1988]. A driving mechanism for Phase 2 is not yet clear. Vaughan [1995] linked mid-Cretaceous deformation in the Antarctic Peninsula and elsewhere to a major, short-lived phase of tectonism affecting Pacific margins and possibly caused by changes in spreading rate and thermal age of oceanic lithosphere associated with the mid-Cretaceous superplume event of Larson [1991a, 1991b]. Although speculative and outside the scope of this manuscript, it seems clear that Phase 2 of the Palmer Land Event, and not Phase 1, may be the local expression of this Pacific-wide event.

### 6.4. Plate Kinematics and the Phases of the Palmer Land Event

[53] While we have shown that the Western and Central Domains could have found their way into collision on either the Phoenix plate or the South American plate, only the latter of these possibilities is consistent with the evidence that parts of these domains may have shared sources of glacial and marine sedimentary rocks, and formed part of common metamorphic and volcanic provinces with southern Patagonia in pre-Cretaceous times [e.g., Barbeau et al., 2010; Bradshaw et al., 2012; Hervé et al., 2006; Riley et al., 2010]. The intraoceanic character of the Central Domain, on the other hand, can be seen as consistent with either scenario. In the light of all this, we would not want to rule out the possibility of mixed provenances and complex pre-collisional histories, involving both the Phoenix and South American plates, for the various components of the Western and Central Domains.

[54] The analysis presented here represents progress in understanding the 107 Ma phase of the Palmer Land Event,

but the later phase remains less well understood. None of the regional plate tectonic settings we have analyzed is simply consistent with the 103 Ma phase of shortening, orthogonal to the 107 Ma phase, developed along 259.5°. The evidence for this phase overprints evidence for the 107 Ma phase, and is confined to the central swath of Palmer Land between 68°S and 74°S (Figure 11). As such, Phase 2 may yet come to be interpretable in terms of modification of the collision zone by the arrival of a local indenter, which remains to be identified. On the other hand, the identification of wide-spread Mesozoic ESE to SSE convergence at the southwest paleo-Pacific margin of Gondwana as outlined above, suggests an additional intra-Pacific influence on the Palmer Land Event that should not be discounted.

## 7. Summary and Conclusions

[55] 1. The Palmer Land Event appears to have had two kinematic phases. Phase 1 was a pure shear shortening to sinistral transpressional phase at ~107 Ma with a principal paleostrain axis of 341°, which is expressed widely along the Antarctic Peninsula but shows its most extensive development in southern Palmer Land. Phase 2 was a pure shear shortening to dextral transpressional phase at ~103 Ma, primarily expressed along the EPLSZ, with a principal paleostrain axis of 259.5°, which is confined to areas between 68°S and 74°S. The evidence suggests that extreme changes in finite strain axis occurred in less than 4 million years.

[56] 2. The kinematics of Phase 1 help to reconcile previously identified apparent differences in strain kinematics on the West Gondwana margin between dextral in the Antarctic Peninsula and sinistral in southern South America in the Mesozoic, by indicating that sinistral kinematics prevailed along this sector of the margin.

[57] 3. The end of Phase 2 marks the end of Mesozoic compressional deformation in the southern Antarctic Peninsula.

[58] 4. The apparent strong strike swing in the southern Antarctic Peninsula results from the superposition of structures from the two phases of the Palmer Land Event, forming an intersection orocline, and not from vertical axis rotation during a single event, so-called oroclinal bending. A peak in LCIS magma emplacement rate was coeval with Phase 1, whereas Phase 2 may have coincided with a lull, suggesting some kinematic control on LCIS emplacement.

[59] 5. Current plate kinematic models for the region suggest plausible alternative scenarios for delivery of the Central and Western Domains into collision with the Eastern Domain along the EPLSZ during Phase 1. The Central and Western Domains may have been carried into the region on board the Phoenix plate or on board the South American plate. Currently available variable provenance indicators from the Central and Western terranes can be cited to support either, or a combination, of these scenarios.

[60] 6. The convergence direction evident from Phase 2 structures is not represented in current models of Phoenix, Antarctic and South American plate kinematics. Together with the confinement of Phase 2 structures to a short length of paleo-plate boundary, this suggests Phase 2 processes were not the result of changes in regional plate kinematics.

[61] 7. Lateral changes in onshore evidence for transpression along the zone of collision for the Palmer Land Event during Phase 1 are primarily a function of the relative

orientation of primary structures and plate tectonic convergence, and may not need to be interpreted in terms of refinements to the regional plate kinematic models.

[62] **Acknowledgments.** This research was funded from British Antarctic Survey Polar Science for Planet Earth core funds as part of the Continental Interiors and LTMS work packages of the Environmental Change and Evolution program. A.P.M.V. would like to thank BAS operations and logistics staff for support while in the field. G.E. thanks Royal Holloway, University of London, for funding. The authors would like to thank Dave Barbeau and Christine Siddoway for insightful and very constructive reviews and would also like to thank the Editor, Onno Oncken, for his assistance.

## References

- Arancibia, G. (2004), Mid-Cretaceous crustal shortening: Evidence from a regional-scale ductile shear zone in the Coastal Range of central Chile (32 degrees S), *J. South Am. Earth Sci.*, 17(3), 209–226, doi:10.1016/j.jsames.2004.06.001.
- Argand, E. (1924), La tectonique de l'Asie, in *Proceedings of the 13th International Geological Congress 1922*, edited by A. Renier, pp. 171–372, Vaillant-Carmann, Liege, Belgium.
- Barbeau, D. L., J. T. Davis, K. E. Murray, V. Valencia, G. E. Gehrels, K. M. Zahid, and D. J. Gombosi (2010), Detrital-zircon geochronology of the metasedimentary rocks of north-western Graham Land, *Antarct. Sci.*, 22, 65–78, doi:10.1017/S095410200999054X.
- Bell, A. C., and E. C. King (1998), New seismic data support Cenozoic rifting in George VI Sound, Antarctic Peninsula, *Geophys. J. Int.*, 134, 889–902, doi:10.1046/j.1365-246x.1998.00605.x.
- Biggin, A. J., and D. N. Thomas (2003), Analysis of long-term variations in the geomagnetic poloidal field intensity and evaluation of their relationship with global geodynamics, *Geophys. J. Int.*, 152, 392–415, doi:10.1046/j.1365-246X.2003.01849.x.
- Bradshaw, J. D., A. P. M. Vaughan, I. L. Millar, M. J. Flowerdew, R. A. J. Trouw, C. M. Fanning, and M. J. Whitehouse (2012), Permo-Carboniferous conglomerates in the Trinity Peninsula Group at View Point, Antarctic Peninsula: Sedimentology, geochronology and isotope evidence for provenance and tectonic setting in Gondwana, *Geol. Mag.*, doi:10.1017/S001675681100080X, in press.
- Cembrano, J., E. Schermer, A. Lavenu, and A. Sanhueza (2000), Contrasting nature of deformation along an intra-arc shear zone, the Liquine-Ofqui fault zone, southern Chilean Andes, *Tectonophysics*, 319(2), 129–149, doi:10.1016/S0040-1951(99)00321-2.
- de Saint Blanquat, M., E. Horsman, G. Habert, S. Morgan, O. Vanderhaeghe, R. Law, and B. Tikoff (2011), Multiscale magmatic cyclicity, duration of pluton construction, and the paradoxical relationship between tectonism and plutonism in continental arcs, *Tectonophysics*, 500(1–4), 20–33, doi:10.1016/j.tecto.2009.12.009.
- Doubleday, P. A., and B. C. Storey (1998), Deformation history of a Mesozoic forearc basin sequence on Alexander Island, Antarctic Peninsula, *J. South Am. Earth Sci.*, 11, 1–21, doi:10.1016/S0895-9811(97)00032-1.
- Doubleday, P. A., and T. H. Tranter (1994), Deformation mechanism paths for oceanic rocks during subduction and accretion: The Mesozoic fore-arc of Alexander-Island, Antarctica, *J. Geol. Soc.*, 151, 543–554, doi:10.1144/gsjgs.151.3.0543.
- Doubleday, P. A., D. I. M. Macdonald, and P. A. R. Nell (1993), Sedimentology and structure of the trench-slope to fore-arc basin transition in the Mesozoic of Alexander Island, Antarctica, *Geol. Mag.*, 130, 737–754, doi:10.1017/S0016756800023128.
- Eagles, G., and A. P. M. Vaughan (2009), Gondwana breakup and plate kinematics: Business as usual, *Geophys. Res. Lett.*, 36, L10302, doi:10.1029/2009GL037552.
- Eagles, G., K. Gohl, and R. D. Larter (2004), High-resolution animated tectonic reconstruction of the South Pacific and West Antarctic margin, *Geochem. Geophys. Geosyst.*, 5, Q07002, doi:10.1029/2003GC000657.
- Farrar, E., S. L. McBride, and P. D. Rowley (1982), Ages and tectonic implications of Andean plutonism in the southern Antarctic Peninsula, in *Antarctic Geoscience*, edited by C. Craddock, pp. 349–356, Univ. of Wis. Press, Madison.
- Ferraccioli, F., P. C. Jones, A. P. M. Vaughan, and P. T. Leat (2006), New aerogeophysical view of the Antarctic Peninsula: More pieces, less puzzle, *Geophys. Res. Lett.*, 33, L05310, doi:10.1029/2005GL024636.
- Ferris, J. K., A. P. M. Vaughan, and E. C. King (2002), A window on West Antarctic crustal boundaries: The junction between the Antarctic Peninsula, the Filchner Block, and Weddell Sea oceanic lithosphere, *Tectonophysics*, 347(1–3), 13–23, doi:10.1016/S0040-1951(01)00235-9.

- Fisher, N. L., T. L. Lewis, and B. J. J. Embleton (1987), *Statistical Analysis of Spherical Data*, 329 pp., Cambridge Univ. Press, Cambridge, U. K., doi:10.1017/CBO9780511623059.
- Flinn, D. (1965), On the symmetry principle and the deformation ellipsoid, *Geol. Mag.*, *102*, 36–45, doi:10.1017/S0016756800053851.
- Flowerdew, M. J., I. L. Millar, A. P. M. Vaughan, and R. J. Pankhurst (2005), Age and tectonic significance of the Lassiter Coast Intrusive Suite, Eastern Ellsworth Land, Antarctic Peninsula, *Antarct. Sci.*, *17*, 443–452, doi:10.1017/S0954102005002877.
- Flowerdew, M. J., I. L. Millar, A. P. M. Vaughan, M. S. A. Horstwood, and C. M. Fanning (2006), The source of granitic gneisses and migmatites in the Antarctic Peninsula: A combined U-Pb SHRIMP and laser ablation Hf isotope study of complex zircons, *Contrib. Mineral. Petrol.*, *151*(6), 751–768, doi:10.1007/s00410-006-0091-6.
- Gee, C. T. (1989), Permian Glossopteris and Elatocladus megafossil floras from the English Coast, eastern Ellsworth Land, Antarctica, *Antarct. Sci.*, *1*, 35–44, doi:10.1017/S0954102089000076.
- Glazner, A. F. (1991), Plutonism, oblique subduction, and continental growth: An example from the Mesozoic of California, *Geology*, *19*(8), 784–786, doi:10.1130/0091-7613(1991)019<0784:POSACG>2.3.CO;2.
- Gradstein, F. M., et al. (2004), *A Geologic Time Scale 2004*, 500 pp., Cambridge Univ. Press, Cambridge, U. K., doi:10.4095/215638.
- Grunow, A. M. (1993), New paleomagnetic data from the Antarctic Peninsula and their tectonic implications, *J. Geophys. Res.*, *98*, 13,815–13,833, doi:10.1029/93JB01089.
- Hamilton, W. B. (1967), Tectonics of Antarctica, *Tectonophysics*, *4*(4–6), 555–568, doi:10.1016/0040-1951(67)90019-4.
- Hathway, B. (2000), Continental rift to back-arc basin: Jurassic–Cretaceous stratigraphical and structural evolution of the Larsen Basins, Antarctic Peninsula, *J. Geol. Soc.*, *157*(2), 417–432, doi:10.1144/jgs.157.2.417.
- Hervé, F., H. Miller, and C. Pimpirev (2006), Patagonia–Antarctica connections before Gondwana break-up, in *Antarctica: Contributions to Global Earth Sciences*, edited by D. K. Fütterer et al., pp. 217–228, Springer, Berlin.
- Hervé, F., M. Calderon, and V. Faundez (2008), The metamorphic complexes of the Patagonian and Fuegian Andes, *Geol. Acta*, *6*(1), 43–53.
- Hoeppener, R. (1955), Tektonik im Schiefergebirge, *Geol. Rundsch.*, *44*, 26–58, doi:10.1007/BF01802903.
- Holdsworth, B. K., and P. A. R. Nell (1992), Mesozoic radiolarian faunas from the Antarctic Peninsula: Age, tectonic and paleoceanographic significance, *J. Geol. Soc.*, *149*, 1003–1020, doi:10.1144/gsjgs.149.6.1003.
- Hunter, M. A., and D. J. Cantrill (2006), A new stratigraphy for the Latady Basin, Antarctic Peninsula: Part 2, Latady Group and basin evolution, *Geol. Mag.*, *143*, 797–819, doi:10.1017/S0016756806002603.
- Hunter, M. A., T. R. Riley, D. J. Cantrill, M. J. Flowerdew, and I. L. Millar (2006), A new stratigraphy for the Latady Basin, Antarctic Peninsula: Part 1, Ellsworth Land Volcanic Group, *Geol. Mag.*, *143*, 777–796, doi:10.1017/S0016756806002597.
- Kellogg, K. S. (1980), Paleomagnetic evidence for oroclinal bending of the southern Antarctic Peninsula, *Geol. Soc. Am. Bull.*, *91*(7), 414–420, doi:10.1130/0016-7606(1980)91<414:PEFOBO>2.0.CO;2.
- Kellogg, K. S., and P. D. Rowley (1989), Structural geology and tectonics of the Orville Coast region, southern Antarctica Peninsula, Antarctica, *U.S. Geol. Surv. Prof. Pap.*, *1498*, 25 pp.
- Kelly, S. R. A., P. A. Doubleday, C. H. C. Brunton, J. M. Dickins, G. D. Sevastopulo, and P. D. Taylor (2001), First Carboniferous and ?Permian marine macrofaunas from Antarctica and their tectonic implications, *J. Geol. Soc.*, *158*(2), 219–232, doi:10.1144/jgs.158.2.219.
- King, E. C., and A. C. Bell (1996), New seismic data from the Ronne Ice Shelf, Antarctica, in *Weddell Sea Tectonics and Gondwana Break-up*, edited by B. C. Storey, E. C. King, and R. A. Livermore, *Geol. Soc. Lond. Spec. Publ.*, *108*, 213–226, doi:10.1144/GSL.SP.1996.108.01.16.
- Koppers, A. A. P., H. Staudigel, J. R. Wijbrans, and M. S. Pringle (1998), The Magellan seamount trail: Implications for Cretaceous hotspot volcanism and absolute Pacific plate motion, *Earth Planet. Sci. Lett.*, *163*(1–4), 53–68, doi:10.1016/S0012-821X(98)00175-7.
- Kraemer, P. E. (2003), Orogenic shortening and the origin of the Patagonian orocline (56°S), *J. South Am. Earth Sci.*, *15*(7), 731–748, doi:10.1016/S0895-9811(02)00132-3.
- Larson, R. L. (1991a), Geological consequences of superplumes, *Geology*, *19*(10), 963–966, doi:10.1130/0091-7613(1991)019<0963:GCOS>2.3.CO;2.
- Larson, R. L. (1991b), Latest pulse of Earth: Evidence for a mid-Cretaceous superplume, *Geology*, *19*(6), 547–550, doi:10.1130/0091-7613(1991)019<0547:LPOEFF>2.3.CO;2.
- Larson, R. L. (1995), The mid-Cretaceous superplume episode, *Sci. Am.*, *272*(2), 82–86, doi:10.1038/scientificamerican0295-82.
- Larson, R. L., R. A. Pockalny, R. F. Viso, E. Erba, L. J. Abrams, B. P. Luyendyk, J. M. Stock, and R. W. Clayton (2002), Mid-Cretaceous tectonic evolution of the Tongareva triple junction in the southwestern Pacific Basin, *Geology*, *30*(1), 67–70, doi:10.1130/0091-7613(2002)030<0067:MCTEOT>2.0.CO;2.
- Larter, R. D., A. P. Cunningham, P. F. Barker, K. Gohl, and F. O. Nitsche (2002), Tectonic evolution of the Pacific margin of Antarctica 1. Late Cretaceous tectonic reconstructions, *J. Geophys. Res.*, *107*(B12), 2345, doi:10.1029/2000JB000052.
- Laudon, T. S. (1991), Petrology of sedimentary rocks from the English Coast, eastern Ellsworth Land, in *Geological Evolution of Antarctica*, edited by M. R. A. Thomson et al., pp. 455–460, Cambridge Univ. Press, Cambridge, U. K.
- Laudon, T. S., and A. B. Ford (1997), Provenance and tectonic setting of sedimentary rocks from eastern Ellsworth Land based on geochemical indicators and sandstone modes, in *The Antarctic Region: Geological Evolution and Processes*, edited by C. A. Ricci, pp. 417–427, Terra Antarc., Siena, Italy.
- Leat, P. T., M. J. Flowerdew, T. R. Riley, M. J. Whitehouse, J. H. Scarrow, and I. L. Millar (2009), Zircon U-Pb dating of Mesozoic volcanic and tectonic events in north-west Palmer Land and south-west Graham Land, Antarctica, *Antarct. Sci.*, *21*, 633–641, doi:10.1017/S0954102009990320.
- Ludwig, K. R. (2003), User manual for isoplot 3.00: A geochronological toolkit for Microsoft Excel, *Berkeley Geochronol. Cent. Spec. Publ.*, *4*, 70 pp., Berkeley Geochronol. Cent., Berkeley, Calif.
- Macdonald, D. I. M., P. T. Leat, P. A. Doubleday, and S. R. A. Kelly (1999), On the origin of fore-arc basins: New evidence of formation by rifting from the Jurassic of Alexander Island, Antarctica, *Terra Nova*, *11*(4), 186–193, doi:10.1046/j.1365-3121.1999.00244.x.
- Marshak, S., and J. R. Tabor (1989), Structure of the Kingston orocline in the Appalachian fold-thrust belt, New York, *Geol. Soc. Am. Bull.*, *101*(5), 683–701, doi:10.1130/0016-7606(1989)101<0683:SOTKIOI>2.3.CO;2.
- McFadden, R. R., C. S. Siddoway, C. Teyssier, and C. M. Fanning (2010), Cretaceous oblique extensional deformation and magma accumulation in the Fosdick Mountains migmatite-cored gneiss dome, West Antarctica, *Tectonics*, *29*, TC4022, doi:10.1029/2009TC002492.
- Meneilly, A. W. (1983), Deformation of granitic plutons in eastern Palmer Land, *Br. Antarct. Surv. Bull.*, *61*, 75–79.
- Meneilly, A. W. (1988), Reverse-fault step at Engel Peaks, Antarctic Peninsula, *J. Struct. Geol.*, *10*(4), 393–403, doi:10.1016/0191-8141(88)90017-X.
- Meneilly, A. W., S. M. Harrison, B. A. Piercy, and B. C. Storey (1987), Structural evolution of the magmatic arc in northern Palmer Land, Antarctic Peninsula, in *Gondwana Six: Structure, Tectonics and Geophysics*, *Geophys. Monogr. Ser.*, vol. 40, edited by G. D. McKenzie, pp. 209–219, AGU, Washington, D. C., doi:10.1029/GM040p0209.
- Millar, I. L., and R. J. Pankhurst (1987), Rb–Sr geochronology of the region between the Antarctic Peninsula and the Transantarctic Mountains: Haag Nunataks and Mesozoic granitoids, in *Gondwana Six: Structure, Tectonics and Geophysics*, *Geophys. Monogr. Ser.*, vol. 40, edited by G. D. McKenzie, pp. 151–160, AGU, Washington, D. C., doi:10.1029/GM040p0151.
- Millar, I. L., R. J. Pankhurst, and C. M. Fanning (2002), Basement chronology of the Antarctic Peninsula: Recurrent magmatism and anatexis in the Palaeozoic Gondwana margin, *J. Geol. Soc.*, *159*(2), 145–157, doi:10.1144/0016-764901-020.
- Müller, R. D., J. Y. Royer, and L. A. Lawver (1993), Revised plate motions relative to the hotspots from combined Atlantic and Indian ocean hotspot tracks, *Geology*, *21*(3), 275–278, doi:10.1130/0091-7613(1993)021<0275:RPMRTT>2.3.CO;2.
- Pankhurst, R. J. (1983), Rb–Sr constraints on the ages of basement rocks of the Antarctic Peninsula, in *Antarctic Earth Science*, edited by R. L. Oliver, P. R. James, and J. B. Jago, pp. 367–373, Cambridge Univ. Press, Cambridge, U. K.
- Pankhurst, R. J., and P. D. Rowley (1991), Rb–Sr study of Cretaceous plutons from southern Antarctic Peninsula and eastern Ellsworth Land, Antarctica, in *Geological Evolution of Antarctica*, edited by M. R. A. Thomson, J. A. Crame, and J. W. Thomson, pp. 387–394, Cambridge Univ. Press, Cambridge, U. K.
- Passchier, C. W., and C. Simpson (1986), Porphyroclast systems as kinematic indicators, *J. Struct. Geol.*, *8*(8), 831–843, doi:10.1016/0191-8141(86)90029-5.
- Poblete, F., C. Arriagada, P. Roperch, N. Astudillo, F. Herve, S. Kraus, and J. P. Le Roux (2011), Paleomagnetism and tectonics of the South Shetland Islands and the northern Antarctic Peninsula, *Earth Planet. Sci. Lett.*, *302*(3–4), 299–313, doi:10.1016/j.epsl.2010.12.019.
- Riley, T. R., and P. T. Leat (1999), Large volume silicic volcanism along the proto-Pacific margin of Gondwana: Lithological and stratigraphical investigations from the Antarctic Peninsula, *Geol. Mag.*, *136*, 1–16, doi:10.1017/S0016756899002265.

- Riley, T. R., P. T. Leat, R. J. Pankhurst, and C. Harris (2001), Origins of large volume rhyolitic volcanism in the Antarctic Peninsula and Patagonia by crustal melting, *J. Petrol.*, 42(6), 1043–1065, doi:10.1093/ptrology/42.6.1043.
- Riley, T. R., M. J. Flowerdew, M. A. Hunter, and M. J. Whitehouse (2010), Middle Jurassic rhyolite volcanism of eastern Graham Land, Antarctic Peninsula: Age correlations and stratigraphic relationships, *Geol. Mag.*, 147, 581–595, doi:10.1017/S0016756809990720.
- Röller, K., and C. A. Trepmann (2003), Stereo32, software, Ruhr-Univ. Bochum, Bochum, Germany. [Available at <http://www.ruhr-uni-bochum.de/hardrock/downloads.html>.]
- Rowley, P. D., W. R. Vennum, K. S. Kellogg, T. S. Laudon, P. E. Carrara, J. M. Boyles, and M. R. A. Thomson (1983), Geology and plate tectonic setting of the Orville Coast and eastern Ellsworth Land, Antarctica, in *Antarctic Earth Science*, edited by R. L. Oliver, P. R. James, and J. B. Jago, pp. 339–348, Aust. Acad. of Sci., Canberra, ACT, Australia.
- Rowley, P. D., E. Farrar, P. E. Carrara, W. R. Vennum, and K. S. Kellogg (1988), Porphyry-type copper deposits and potassium-argon ages of plutonic rocks of the Orville Coast and eastern Ellsworth Land, Antarctica, in *Studies of the Geology and Mineral Resources of the Southern Antarctic Peninsula and Eastern Ellsworth Land, Antarctica*, edited by P. D. Rowley and W. R. Vennum, *U.S. Geol. Surv. Prof. Pap.*, 1351, 35–49.
- Sager, W. W. (2006), Cretaceous paleomagnetic apparent polar wander path for the Pacific plate calculated from Deep Sea Drilling Project and Ocean Drilling Program basalt cores, *Phys. Earth Planet. Inter.*, 156(3–4), 329–349, doi:10.1016/j.pepi.2005.09.014.
- Scarrow, J. H., A. P. M. Vaughan, and P. T. Leat (1997), Ridge-trench collision-induced switching of arc tectonics and magma sources: Clues from Antarctic Peninsula mafic dykes, *Terra Nova*, 9(5–6), 255–259, doi:10.1111/j.1365-3121.1997.tb00024.x.
- Seton, M., C. Gaina, R. D. Muller, and C. Heine (2009), Mid-Cretaceous seafloor spreading pulse: Fact or fiction?, *Geology*, 37(8), 687–690, doi:10.1130/G25624A.1.
- Sharp, W. D., O. T. Tobisch, and P. R. Renne (2000), Development of Cretaceous transpressional cleavage synchronous with batholith emplacement, central Sierra Nevada, California, *Geol. Soc. Am. Bull.*, 112(7), 1059–1066, doi:10.1130/0016-7606(2000)112<1059:DOCTCS>2.0.CO;2.
- Siddoway, C. S., L. C. Sass III, and R. P. Esser (2005), Kinematic history of the Marie Byrd Land terrane, West Antarctica: Direct evidence from Cretaceous mafic dykes, in *Terrane Processes at the Margins of Gondwana*, edited by A. P. M. Vaughan, P. T. Leat, and R. J. Pankhurst, *Spec. Publ. Geol. Soc.*, 246, 417–438, doi:10.1144/GSL.SP.2005.246.01.17.
- Simpson, C., and D. G. Depaor (1993), Strain and kinematic analysis in general shear zones, *J. Struct. Geol.*, 15(1), 1–20, doi:10.1016/0191-8141(93)90075-L.
- Smellie, J. L. (1981), A complete arc-trench system recognized in Gondwana sequences of the Antarctic Peninsula region, *Geol. Mag.*, 118, 139–159, doi:10.1017/S001675680003435X.
- Storey, B. C., and S. W. Garrett (1985), Crustal growth of the Antarctic Peninsula by accretion, magmatism and extension, *Geol. Mag.*, 122, 5–14, doi:10.1017/S0016756800034038.
- Storey, B. C., and P. A. R. Nell (1988), Role of strike-slip faulting in the tectonic evolution of the Antarctic Peninsula, *J. Geol. Soc.*, 145(2), 333–337, doi:10.1144/gsjgs.145.2.0333.
- Storey, B. C., H. E. Wever, P. D. Rowley, and A. B. Ford (1987), Report on Antarctic fieldwork: The geology of the central Black Coast, eastern Palmer Land, *Br. Antarct. Surv. Bull.*, 77, 145–155.
- Storey, B. C., R. W. Brown, A. Carter, P. A. Doubleday, A. J. Hurford, D. I. M. Macdonald, and P. A. R. Nell (1996), Fission-track evidence for the thermotectonic evolution of a Mesozoic–Cenozoic fore-arc, Antarctica, *J. Geol. Soc.*, 153(1), 65–82, doi:10.1144/gsjgs.153.1.0065.
- Suárez, M. (1976), Plate tectonic model for southern Antarctic Peninsula and its relation to southern Andes, *Geology*, 4(4), 211–214, doi:10.1130/0091-7613(1976)4<211:PMFSAP>2.0.CO;2.
- Sutherland, R., and C. Hollis (2001), Cretaceous demise of the Moa plate and strike-slip motion at the Gondwana margin, *Geology*, 29(3), 279–282, doi:10.1130/0091-7613(2001)029<0279:CDOTMP>2.0.CO;2.
- Trouw, R. A. J., C. W. Passchier, C. M. Valeriano, L. S. A. Simoes, F. V. P. Paciullo, and A. Ribeiro (2000), Deformational evolution of a Cretaceous subduction complex: Elephant Island, South Shetland Islands, Antarctica, *Tectonophysics*, 319(2), 93–110, doi:10.1016/S0040-1951(00)00021-4.
- Vaughan, A. P. M. (1995), Circum-Pacific mid-Cretaceous deformation and uplift: A superplume-related event?, *Geology*, 23(6), 491–494, doi:10.1130/0091-7613(1995)023<0491:CPMCDA>2.3.CO;2.
- Vaughan, A. P. M., and R. A. Livermore (2005), Episodicity of Mesozoic terrane accretion along the Pacific margin of Gondwana: Implications for superplume-plate interactions, in *Terrane Processes at the Margins of Gondwana*, edited by A. P. M. Vaughan, P. T. Leat, and R. J. Pankhurst, *Spec. Publ. Geol. Soc.*, 246, 143–178, doi:10.1144/GSL.SP.2005.246.01.05.
- Vaughan, A. P. M., and R. J. Pankhurst (2008), Tectonic overview of the West Gondwana margin, *Gondwana Res.*, 13(2), 150–162, doi:10.1016/j.gr.2007.07.004.
- Vaughan, A. P. M., and B. C. Storey (1997), Mesozoic geodynamic evolution of the Antarctic Peninsula, in *The Antarctic Region: Geological Evolution and Processes*, edited by C. A. Ricci, pp. 373–382, Terra Antarc., Siena, Italy.
- Vaughan, A. P. M., and B. C. Storey (2000), The eastern Palmer Land shear zone: A new terrane accretion model for the Mesozoic development of the Antarctic Peninsula, *J. Geol. Soc.*, 157(6), 1243–1256, doi:10.1144/jgs.157.6.1243.
- Vaughan, A. P. M., I. L. Millar, and L. Thistlewood (1999), The Auriga Nunataks shear zone: Mesozoic transfer faulting and arc deformation in northwest Palmer Land, Antarctica, *Tectonics*, 18(5), 911–928, doi:10.1029/1999TC900008.
- Vaughan, A. P. M., R. J. Pankhurst, and C. M. Fanning (2002a), A mid-Cretaceous age for the Palmer Land event, Antarctic Peninsula: Implications for terrane accretion timing and Gondwana palaeolatitudes, *J. Geol. Soc.*, 159(2), 113–116, doi:10.1144/0016-7649a101-090.
- Vaughan, A. P. M., S. P. Kelley, and B. C. Storey (2002b), Mid-Cretaceous ductile deformation on the Eastern Palmer Land Shear Zone, Antarctica, and implications for timing of Mesozoic terrane collision, *Geol. Mag.*, 139, 465–471, doi:10.1017/S0016756802006672.
- Vaughan, A. P. M., P. T. Leat, and R. J. Pankhurst (2005), Terrane processes at the margins of Gondwana: Introduction, in *Terrane Processes at the Margins of Gondwana*, edited by A. P. M. Vaughan, P. T. Leat, and R. J. Pankhurst, *Spec. Publ. Geol. Soc.*, 246, 1–22, doi:10.1144/GSL.SP.2005.246.01.01.
- Vennum, W. R., and P. D. Rowley (1986), Reconnaissance geochemistry of the Lassiter Coast Intrusive Suite, southern Antarctic Peninsula, *Geol. Soc. Am. Bull.*, 97(12), 1521–1533, doi:10.1130/0016-7606(1986)97<1521:RGOTLC>2.0.CO;2.
- Wareham, C. D., I. L. Millar, and A. P. M. Vaughan (1997), The generation of sodic granite magmas, western Palmer Land, Antarctic Peninsula, *Contrib. Mineral. Petrol.*, 128(1), 81–96, doi:10.1007/s004100050295.
- Wareham, C. D., R. J. Pankhurst, R. J. Thomas, B. C. Storey, G. H. Grantham, J. Jacobs, and B. M. Eglinton (1998), Pb, Nd, and Sr isotope mapping of Grenville-age crustal provinces in Rodinia, *J. Geol.*, 106(6), 647–660, doi:10.1086/516051.
- Wendt, A. S., A. P. M. Vaughan, and A. J. Tate (2008), Metamorphic rocks in the Antarctic Peninsula region, *Geol. Mag.*, 145, 655–676, doi:10.1017/S0016756808005050.
- Wever, H. E., I. L. Millar, and R. J. Pankhurst (1994), Geochronology and radiogenic isotope geology of Mesozoic rocks from eastern Palmer Land, Antarctic Peninsula: Crustal anatexis in arc-related granitoid genesis, *J. South Am. Earth Sci.*, 7(1), 69–83, doi:10.1016/0895-9811(94)90035-3.
- Wever, H. E., B. C. Storey, and P. T. Leat (1995), Peraluminous granites in NE Palmer Land, Antarctic Peninsula: Early Mesozoic crustal melting in a magmatic arc, *J. Geol. Soc.*, 152(1), 85–96, doi:10.1144/gsjgs.152.1.0085.
- Whitham, A. G., and B. C. Storey (1989), Late Jurassic–Early Cretaceous strike-slip deformation in the Nordenskjöld Formation of Graham Land, *Antarct. Sci.*, 1, 269–278, doi:10.1017/S0954102089000398.
- Willan, R. C. R. (2003), Provenance of Triassic–Cretaceous sandstones in the Antarctic Peninsula: Implications for terrane models during Gondwana breakup, *J. Sediment. Res.*, 73(6), 1062–1077, doi:10.1306/050103731062.
- Worthington, T. J., R. Hekinian, P. Stoffers, T. Kuhn, and F. Hauff (2006), Osborn Trough: Structure, geochemistry and implications of a mid-Cretaceous paleosubduction ridge in the South Pacific, *Earth Planet. Sci. Lett.*, 245(3–4), 685–701, doi:10.1016/j.epsl.2006.03.018.
- Yeh, M. W., and T. H. Bell (2004), Significance of dextral reactivation of an E-W transfer fault in the formation of the Pennsylvania orocline, central Appalachians, *Tectonics*, 23, TC5009, doi:10.1029/2003TC001593.

G. Eagles, Department of Earth Sciences, Royal Holloway, University of London, Egham TW20 0EX, UK. (g.eagles@es.rhul.ac.uk)

M. J. Flowerdew and A. P. M. Vaughan, British Antarctic Survey, High Cross, Madingley Road, Cambridge CB3 0ET, UK. (alan.vaughan@bas.ac.uk)